社会開発協力部報告書

RESEARCH REPORT ON THE INVESTIGATION OF LANDSLIDE AND SOIL EROSION IN NEPAL USING REMOTE SENSING TECHNOLOGYY

MARCH 1996

JAPAN INTERNATIONAL COOPERATION AGENCY
JAPAN SOCIETY OF EROSION CONTRO ENGINEERING

JAPAN INTERNATIONAL COOPERATION AGENCY
RESEARCH REPORT ON THE INVESTIGATION OF LANDSLIDE AND SOIL EROSION IN NEPAL USING REMOTE SENSING TECHNOLOGY
MARCH 1996
JAPAN SOCIETY OF EROSION CONTRO ENGINEERING

RESEARCH REPORT ON THE INVESTIGATION OF LANDSLIDE AND SOIL EROSION IN NEPAL USING REMOTE SENSING TECHNOLOGYY

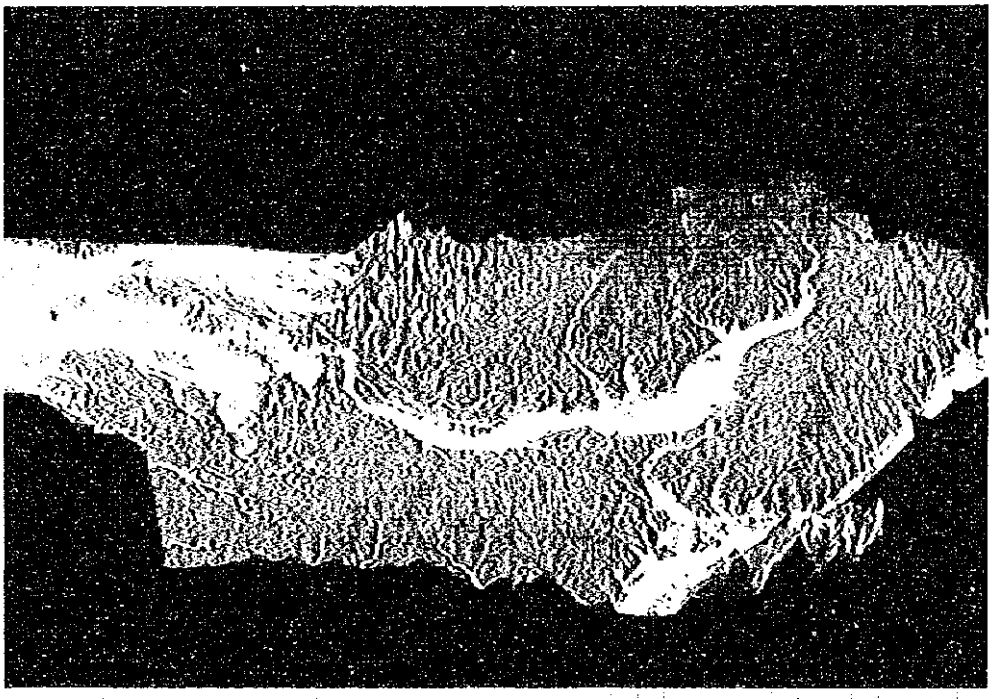

MARCH 1996

JAPAN INTERNATIONAL COOPERATION AGENCY
JAPAN SOCIETY OF EROSION CONTRO ENGINEERING

TABLE OF CONTENTS

LIST OF FIGURES

LIST OF TABLES

CHAPTER 1

INTRODUCTION

CHAPTER I INTRODUCTION

In July 1993 high intensity rainfall occurred in the Central Nepal in two occasions with more than 500mm of rainfall within 24 hours. This rainfall was concentrated in the central hills of Nepal extending from Mahabarth mountain region Siwalik hills and extending to Terai region. This natural phenomena caused heavy toll of damage. The death toll rose to 1460 and about 39495 houses were damaged. The transportation between to and from Katmandu was cutoff for few days hindering timely rescue work for affected people.

A country like Nepal where the road transportation facilities are yet to develop further hinder the development further by sudden calamities like 1993 floods. There is a urgent need in making proper land management to reduce soil erosion hazards, improve watersheds and plan for transportation network with better comprehensive studies.

This research project was aimed at studying the 1993 flood, and its affect on the Ratu watershed to characterize the soil erosion, and transportation and deposition phenomena using satellite remote sensing and GIS technologies. The extension of the developed methodology to Nepal was investigated and active work plan was proposed.

CHAPTER 2

BACKGROUND OF THE PROJECT

CHAPTER 2 BACKGROUND OF THE PROJECT

2.1 Natural Disasters in Nepal

Nepal is a mountainous country, rectangular in shape extending 80E to 88E in NW - SE and 26.3N to 30.4N in the NS direction, of 147,181 square kilometers in area. Two third of the total area of the country is occupied by hills and mountains. Population of stands at 18.8 million (1992), with a growth rate of 2.1%. Ninety percent of the total population is depend on agriculture occupying most of the hill tops and valleys for cultivation. Forest land in the living environment is the fuel reserve for peasants, and food storage for animals that supply supplementary food and money, the nominal income. Forest provide fuelwood, construction materials, fodder for livestock and other products needed by the rural communities on a day-to-day basis. It is estimated that 75% of the total energy comes from forest, Table 2.1.

Table 2.1 Energy supply - 1992 (WECS Report, 1992)

	Terai - Siwalik	Middle Mountain	High Mountain
Forest	48%	90%	76%
Animal Waste	21%	0.10%	18%
Agriculture Residue	23%	9.50%	4.50%

Settling on hill tops and hill slopes is a common practice in Nepal, where the forest land encroachment can be expected with the increase with population. This leads to high degree of degradation of the land and loss of natural forest resources. The changes in the forest cover could have impact on climatic and weather patterns causing intensive rainfall, consequently floods.

The land of Nepal lies in very distinctive geological and ecological zones, Table 2.2. This shows the distinct differences of each zone in their geological and climatic aspect. Also, this indicates the deforestation situation of each region. Terai and Siwalik regions, where the concentration of the population is high has a high ratio of deforestation. This will be prolong unless the increasing population is diverted from cropping pattern that is locally practice present. Sharma, 1978 reported that the demand for forest fuel in 1985

exceeds the availability and this will increase every year. With the increasing population, burden on the forest and in the mean time land itself will increase resulting further land degradation. Loss of forest will have negative impact on the society in the country level, and may have affect on the climate in the global scale. The accelerating number of natural hazards and the their recurrence period would be a good indicator of the environmental degradation experiences in Nepal today. Existing forest cover and its change could be one of the main factor that could influence the occurrence of these natural hazards.

Table 2.2 Geological, Ecological zones and characteristics (Sharma, 1988)

	width km	Area sq. km	Rock type	Climate	Forest 1964 - 1978
Terai	20-50	20580	Alluvium	Sub-Tropical	-24%
Siwalik	20-30	22050	Sandstone	Sub-Tropical	-15%
Midland	40-60	42630	Granite / Schist	Temperate	1.8%
High Mt.	20-30	27930	Granite / Schist	Sub-Alpine	1.8%
High Himals	20-90	33810	Himal Gneiss	Alpine	N/A

The major natural disasters that occur in Nepal are glacier lakes out burst, earthquakes, floods, droughts, landslides, out of which glacier lakes out burst, floods, droughts and landslides are water induced disasters. The causes for these calamities could be natural or man made. Some of the important factors that could induce or influence natural hazards are summarized in Table 2.3.

Table 2.3 Probable causes of triggering hazards

Natural	Man made
Topographical	Grazing
Climatic factors	Terracing
Tectonic forces	Deforestation
Geological formations	Forest fire

Glacier lakes are created by accumulation of debris along the ridges of glacier snout during the melting season. Glaciers and ice-sheets are believed to erode

the material beneath them by abrasion and plucking. The sediment created by fracturing the bedrock and the worn-out particles themselves are transported with and within the glaziers. Much of the sediment load of glacier is removed and deposited during the process of melting. When a glacier is subjected to incoming heat or any other friction, the ice is melted and drained out with finer sediment particles leaving coarse material in the vicinity of glacier face. At the snout of the glacier englacial debris melt out and create a ablation moraine layer protecting the snout from the direct sun rays reducing further melting. As a result the supraglacial lateral and medial moraines grow into ice-cored ridges rising up to 30-40 meters above the glacier surface. Most of these lakes are self draining, but external causes or the water pressure itself could cause the dam to be broken discharging enormous amount of water in a short time causing unprecedented damaged in the down stream.

Nepal is a flood prone country. The reason could be a high intensive rainfall, a glacier lake out burst or damming of a river due to a landslide. The high intensity rainfall is a natural phenomenon that produces large amount of rainfall within a short period of time. In some occasion the amount of rainfall has been exceeded 400mm within 24 hours. This high intensity rainfall, some authors referred to as *cloud burst* are generally occurring in Central and Eastern Nepal. It is reported that Longitude 85 to Longitude 86 is highly susceptible for cloud burst precipitation. The occurrence of high intensity rainfall has increased in recent years and cloud burst floods becoming a frequent event in Central Nepal. Some of the reasons for this phenomenon are topography, elevation and the degree of environmental degradation, but their contribution is yet to identified.

A natural hazard turns into a natural disaster when an event causes in heavy losses to life, property and other economic assets in a society. This mostly happens when human activities on account of limited knowledge, resources, capacities and alternatives, take place in natural hazard prone areas. The importance of land, forest and forest products for the rural people of Nepal can not be overstated, but the harmony between the nature and the human

environment should be maintain by reducing strain on land and forest resources to reduce or avoid unprecedented affect from natural hazards.

Natural events are indicators of changes in seasonal, climatic or biological environment. Nepal extends from Mt. Everest that stands at 8848m to the lower plane of Terai where the average elevation is about 130 meters the climate changes from alpine environment to sub-tropical. Also, the geological formation of the high mountains, Churiya hills and Terai regions belong to different geological ages, and their characteristics are dissimilar. Nature, order, and the consequences of natural disasters like floods, landslides are dependent on many natural variables. Realistic approach for understanding landslides, floods or soil erosion hazards it is advisable to consider areas with similar natural conditions.

2.2 Storm and Flood Hazard in July 1993

There were two major floods occurred in two separate periods in July and August 1993. The July events were occurred around 20-21, and the later one was around 9-10 August. It was reported that the July flood was severe than the damage caused by the August events. Both these events had been occurred in summer, which is a characteristics of floods in Nepal. Also, both of these events are consequence of cloud burst rainfall. During this period the summer monsoon trough was located over the central Nepal between Katmandu and Indian border.

Unusually high intensity precipitation occurred in the upper part of the Mahabharat Range covering three major watersheds Bagmati, Trishuli, and Rapti on July 19, 1993. Further, similar high intensity precipitation was followed in the Siwalik area and the lower part of Mahabharat Range on the following day. This unprecedented rainfall triggered floods and landslides in eastern and Central Nepal causing heavy losses of infrastructure, life and property.

Figure 2.1, 2.2 show the rainfall distribution of the storm. Figure 2.1 shows that rainfall exceeding 500mm were experienced in the middle Bagmati and

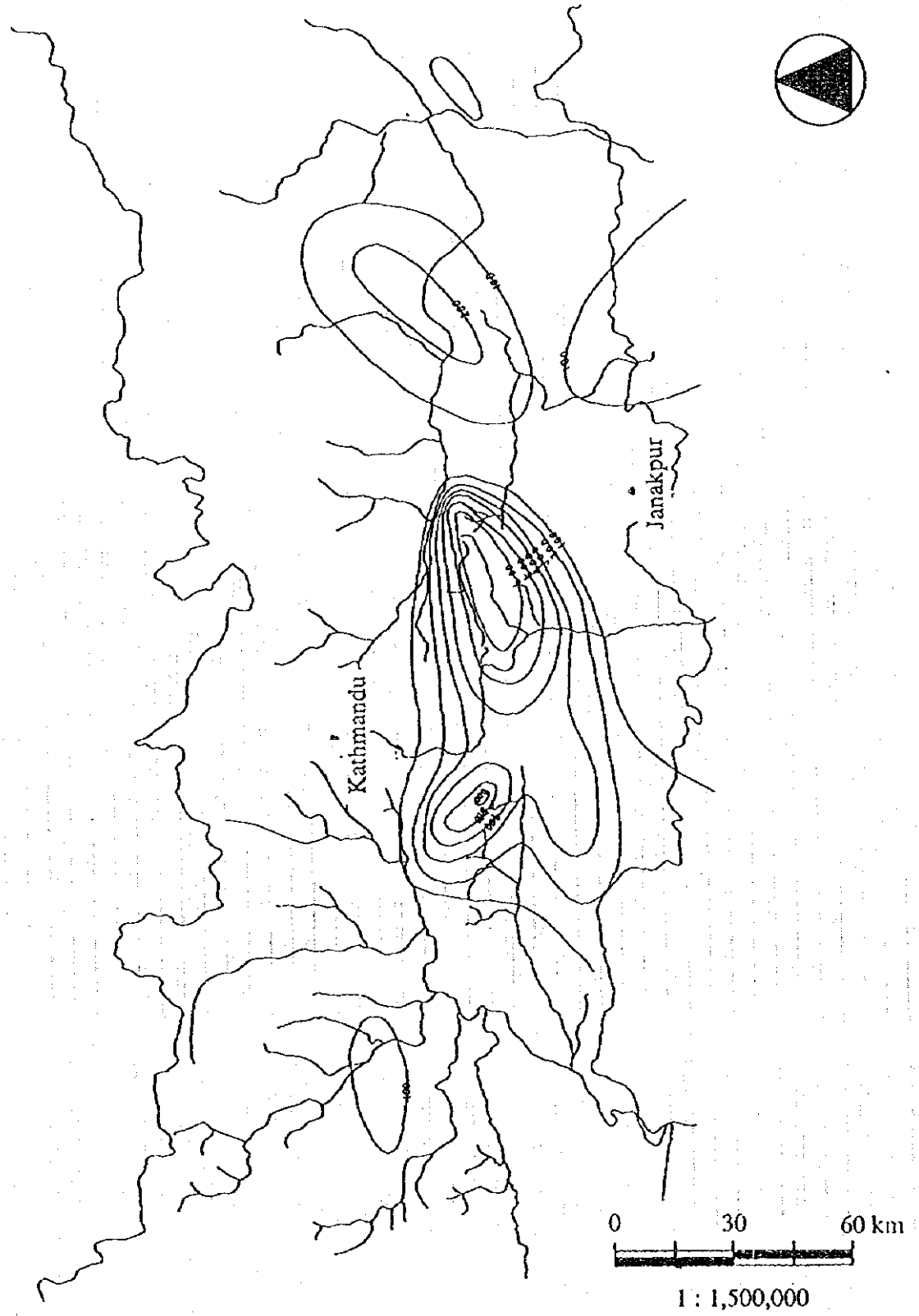

RESEARCH REPORT ON THE INVESTIGATION OF LANDSLIDE AND SOIL EROSION IN NEPAL USING REMOTE SENSING TECHNOLOGY	Figure 2.1 Isohyetal map of 1993 July rainfall (19-21)
	JAPAN INTERNATIONAL COOPERATION AGENCY

the Marin Kola region. Figure 2.2 shows that the rainfalls exceeding 300mm were experienced in the region extending from Nargani to Kamala river basin. The precipitation was concentrated in the central hills and decreased to 100mm in the Terai region.

The volume of precipitation received in the Central Nepal for 24 hour period was about 540mm at the highest place with an average of 350mm. In this area nearly 8000 families, 17 Village Councils were affected by mass movement activities caused by intensive rainfall. It was reported that 160 people died in this area. Further, almost all the bridges located over rives starting from Mahabarth and belongs to Makawannapur and Dhading districts were washed away by the floods.

In the Siwalik area high intensity rainfall was observed in the eastern part of Makawanpur, southern part of Kavre and western part of Sindhuli districts. The maximum rainfall recorded in this area was about 500mm for 24 hours. The affected areas are high both in upper stream and down stream areas where the rivers that originate or flow through Siwalik, and spreads into low plain Terai region. It is reported that 17,000 families are affected, where about 70% were belonged to Sindhuli district in the upper streams. About 35,000 families were affected in the Rautahat and Sarlahi districts in the down stream.

The 1993 July floods is one of the worst in the Nepal history. The total damaged was about 4000 million Nepal Rupees. Table 2.4 shows the findings reported by ICIMOD, 1993.

Table 2.4 Damage by 1993 July floods (ICIMOD, 1993)

Damaged Household	64181
Affected Population	544958
Death	1148
Affected Land in Hectares	43100
Livestock	24968
Bridges	207
Dams	34
Public Buildings	399

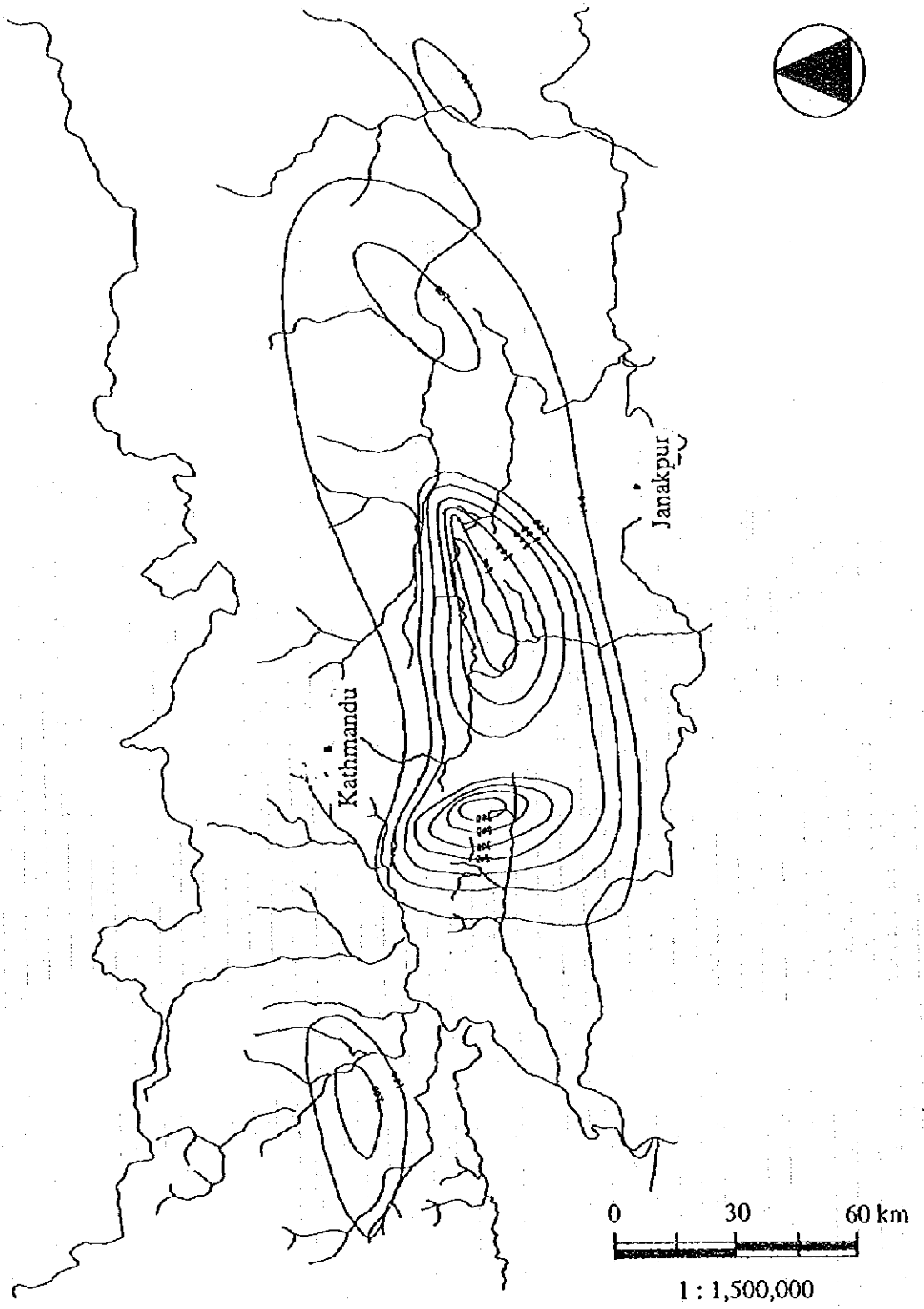

RESEARCH REPORT ON THE INVESTIGATION OF LANDSLIDE AND SOIL EROSION IN NEPAL USING REMOTE SENSING TECHNOLOGY	Figure 2.2 Isohyetal map of 1993 July rainfall (20-21)
	JAPAN INTERNATIONAL COOPERATION AGENCY

Spatial distribution of the affects are thematically shown in Appendix 1. Affected bridges, dams, households, land loss, roads, livestock, deaths are shown in Appendix 1-1 to 1-6.

The above table shows the dramatic damage caused by single event, and the destructive power of high intensive rainfall in this Himalayan country. These types of events may be rarely occurred. Though the probability of occurring an event in this scale could be once in every fifty or hundred years, their impact on life and property is very high. Events that are considered as natural and had little impact on the society are taking heavier tolls today as the flood plains and other marginal lands are cultivated, improved for living environments with little or no concern on the environmental degradation.

Also, the 1993 flood and its affect on the society is summarized in tangible economical units, and affected number of people. The amount of land degradation that may have directly and indirectly supported these devastating effects not be evaluated in monetary values. But the amount of soil loss, and the consequence of it on the society could be enormous. The escalating devastating flood events causes heavier losses by washing away the topsoil. The related consequences are rapid siltation of reservoirs, abrupt changes in the courses of rivers, spread of barren sand and gravel across rich agricultural land on the plain. This would lead to another round of deforestation for crop lands, fuel, fodder further increasing the burden on forest reserves. This further escalate the soil loss and other natural hazards. Ives, 1987 says that in the worst case the top soil which very basis for existence of life will virtually flow down to Bay of Bengal by the year 2000.

2.3 Natural & Human Impact on Flood Hazards

Flood is a consequence of intensive rainfall. Excessive rainfall may not be a major threat unless it increases the surface runoff. Further, the increase in the surface runoff or the overland flow could cause land denudation and floodplain sedimentation once the water flow become influential in eroding and

transporting soil. Therefore, consequences of a flood event could further escalate the degree of denudation by the rate of erodibility of land, and transporting capacity of the stormflow. This geomorphic process could be occur due to soil transport in running water, earthslide, mudflows, rockfalls, talus creep, or avalanches. Occurrence of these activities could be natural or man induced. Underlying bedrock lithology and structure, slope factor, rainfall intensities, earthquakes are some of natural factors that causes or increases the denudation, and deforestation, terracing are some form of human influences on the rate of sedimentation.

Table 2.5 Denudation rates for Himalayan Region (After Ives, 1989)

Location	Denudation mm/year	Comment	Author
Himalaya	1.0	Regional	Menard, 1961
Hunza Watershed	1.8	From Sediment	Ferguson, 1984
Tamur Watershed	5.14	From Sediment	Seshardi, 1960
Tamur Watershed	4.70	From Sediment	Ahuja, 1958
Tamur Watershed	2.56		Williams, 1977
SunKosi Watershed	2.50		Pal, 1974
SunKosi Watershed	1.43		Williams, 1977
Kosi Watershed	0.98		Schumn, 1963
Kosi Watershed	1.00		Williams, 1977
Arun Watershed	1.90		Pal, 1974
Arun Watershed	0.51		Williams, 1977

Exact reasons are not know for the high degree of land degradation in the Siwalik, but most of literature published blaming the farmer for destruction of forest for energy subsidy and mountain farming. Of course these activities also could influence the erodibility, but the natural causes can not be ignored. Ives, 1989 noted that the geophysical and climatic processes may be responsible for high land denudation in this extremely active landscape. Table

2.5 provides selected denudation rates for the Himalaya as a whole and for some major watersheds.

The denudation figures are some what different for same watershed due to differences in estimated methods and the period of evaluation. The cause and the effect of the degradation is very much crucial to bring about proper and timely counter measures, but the information available for the geormorphologicaly unstable Himalayan region is rather limited. The detail examination of sedimentation in watershed basis may be a better solution to understand the cause and effect of the flood and soil erosion process, but the limited resources may hinder this efforts. Further, it would be better to recognize these phenomenon on regional basis and consider detail surveys survey on the areas with the basis of the regional scale findings.

2.4 Objectives of the Project

It could be said that hazardous events in Nepal will continue to occur in the future because of the nature of the environment and the degree of present exploitation of land. The present level of understanding and analysis of natural events are very poor in Nepal. No proper monitoring activities are carried out in regular basis. Lack of knowledge of natural events, their occurrence, recurrence time span could hinder proper planning for disaster prevention, and mitigation. It was thought satellite remote sensing data could offset the information gap as they can provide timely, and repetitive data of a particular phenomena without physically visiting the area of interest.

In this study it was decide to investigate the applicability of satellite data for river management, land degradation assessment and monitor these phenomena. The objectives of the study can be enumerated as below;

- Estimate the river sedimentation and channel planform change using satellite data

- Impact assessment of Floodplain sedimentation on land cover and land use.
- Estimate the change of forest cover that could influence surface erosion using remote sensing technology
- Establish a soil erosion model that comprise parameters easily obtainable from available data or satellite remote sensing
- Investigate the physical nature of soil erosion and sedimentation process to establish sediment budget
- Use of satellite data for comprehensive river management
- proposals to transfer the identified technology of the present research works to Nepal

CHAPTER 3

REMOTE SENSING SYSTEM AND DATA

CHAPTER 3 REMOTE SENSING SYSTEMS AND DATA

Remote sensing is the process that obtain information about an object without making physical contact with it. It could be visualized in two different aspects; the technology of acquiring the data through some form of device which is located away from the object or the phenomena of interest, and the technology that required to analyze the gathered information to interpret the physical attribute of the object. What is observed by human eye to information transferred to us observing from balloons, aircraft, satellites are some of the sensing systems relay information without direct contact with objects. Among them, the newly developed satellite remote sensing technology has become a valuable form of information gathering system for professionals who are dealing with the physical characteristics of earth system.

3.1 Energy Earth Interaction

Remote sensing system constitute with an object, sensing device and information transfer media from object to the sensor. This could be accomplished by the electromagnetic waves which could propagate through the atmosphere and the outer sphere. Most of the land information remote sensing operates by sensing the electromagnetic radiation that is reflected or emitted by earth objects.

Electromagnetic spectrum is the ordering of electromagnetic radiation according to wavelength, or frequency. The order of wavelength frequently represented from cosmic rays to radio waves. The wavelengths in between these two extremities are named as gamma rays, X-rays, ultra-violet, visible, near-infrared, middle-infrared, far-infrared and microwave. For remote sensing purposes the most important spectral regions are 0.4-1.4μm, which is referred to as optical region and the 2mm to 0.8m microwave region. The most common remote sensing systems termed as passive systems measure the intensity of naturally available radiation of the objects. The radiation generating systems working in the micro wave regions are started to exist

before the innovation of present popular passive systems, and they referred to as active sensors.

Passive sensors observe the reflected suns energy from the earth surface and the emitted energy from the earth itself. Due to high temperature of sun compared to that of the earth, energy in the visible spectrum of that receives at the sensor dominated by the reflected energy of sun irradiation. In contrast, the far-infrared region is conceits of energy emitted by the earth, and the middle-infrared van be considered as a combination of reflected of suns radiation and emitted from the earth.

When an electromagnetic energy is incident on any given earth surface feature, three fundamental energy interaction with the feature is possible, Figure 3.1.

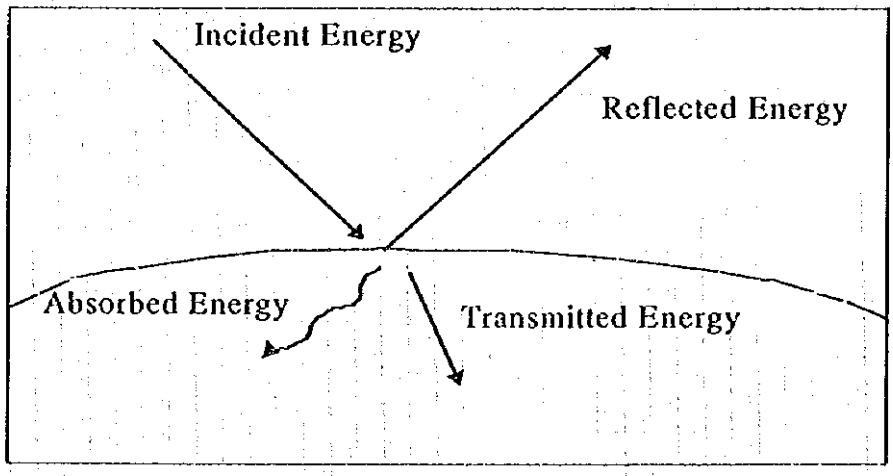

Figure 3.1 Energy Interaction with the earth surface

The fraction of transmitted, reflected, and absorbed energy is a function of the properties of the material type and condition. These differences can be used to identify similar and dissimilar objects on an image. Further, the energy interaction is depend on the wavelength. This refers to the fact that even for a given feature type the reflected, transmitted, and absorbed energy will vary at different wavelength. This facilitates to distinguish objects that have similar spectral response in one spectral range by observing them in different wavelengths.

The physical features on the earth surface can be generalized into four major cover classes, water, vegetation, and soil. Typical spectral curves for these cover classes are shown in Figure 3.2. These curves represents average reflectance curves for these cover types. The spectral patterns of these features at a given locality may deviate from these curves, but may retain their relative distribution unchanged. Vegetation reflectance shows high variability, and the low reflectance in the visible region of the spectrum is account for the pigments in plant leaves. If a plant is subjective to some form of stress or damage that interrupts the growth decreasing the chlorophyll production the spectral reflectance in the red band may increase. In the near-infrared of the spectrum the reflectance of vegetation increases dramatically, primarily due to internal; structure of plants. Further moving into higher wavelengths the reflectance decreases, and two dips in reflectance occur in the highly water absorption regions of the spectrum. In the case of water, the most distinctive characteristic is the energy absorption in the near-infrared wavelengths. In this region water or moisture availability decides the amount of energy absorbed and reflected. In contrast to these two features, the soil spectral behavior is smoother, increasing with the increase of the wavelength. Reflectance of soil could change with change in the moisture condition, texture or surface roughness. Presence of moisture in soil decrease the reflectance, and this could be visible in t5he near-infrared range. Further, the soil texture which is related to soil moisture, where sandy and coarse grained soil may have less moisture and reflect high. Poorly drained fine texture soil may reflect relatively low.

These explanations show that most of the earth features can be identified with remote sensing data. There could be features with similar spectral properties where the separation can not be achieved. For better utilization of remote sensing information it is pre-requisite to understand the spectral characteristics of the feature in consideration and the factors that could influenced or change the spectral properties of the feature.

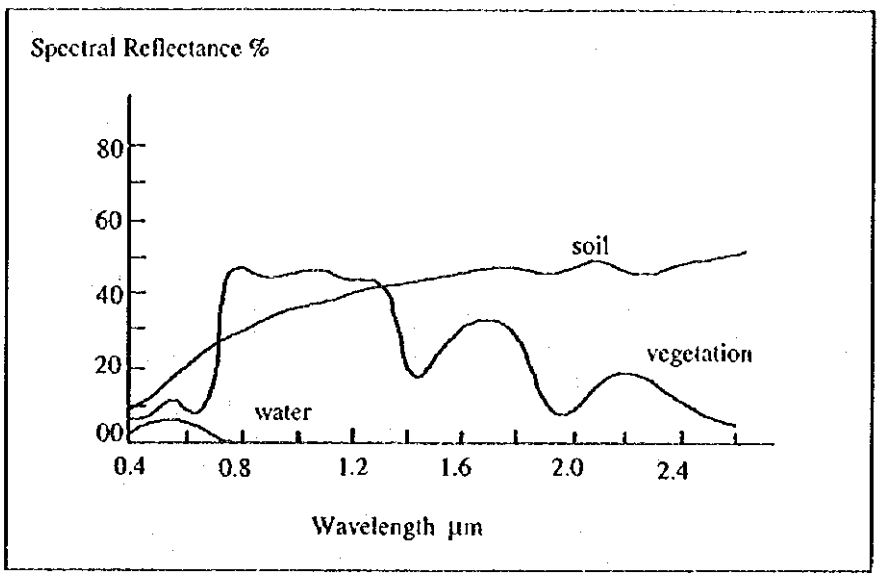

Figure 3.2 Generalized spectral curves of some typical features

3.2 Satellite Systems

Remote sensing form space began in the period 1946 to 1950 when small cameras are carried aboard captured V-2 rockets and the succeeding years numerous flight involving different cameras were launched. The existing remote sensing may have started after receiving photographs from manned spacecraft in 1960. Motivated by the excellent quality of these photographs and those received from successive spacecraft, NASA initiated a program for Earth resources Technology Satellites in 1967. The first satellite, ERTS-1 was launched in 1972, and successive satellite in following years. After launching the first one the program was renamed as Landsat. Launching 6 satellite, shows the success of the Landsat program. At present, only one Landsat-5 is in operation. The mishap of Landsat-6 which was launched in 1995 is real tragedy, but the successive one will be supposed to launched in 1997. Following the success of NASA satellite program, French Government decided to launch their satellite system with the participation of Belgium and Sweden. The SPOT satellite system was launched in 1986 and the follow up satellites are supporting the remote sensing society with their continuous

service. Marine Observation Satellite (MOS), National Oceanic and Atmospheric Administration (NOAA) system, and recently launched radar systems, European Earth Remote Sensing system (ERS) and Japanese Earth Resources Satellite (JERS) series. The main characteristics of these satellites and their sensors are listed in Table 3.1. NOAA gives the best repetition for monitoring with very coarse ground resolution for regional or country level information management. Landsat TM data gives the largest synoptic view with a single data set and it contains number of spectral bands suitable for multi-disciplinary applications. The MOSS data is similar to Landsat MSS in number of bands and the band wavelength, but has the poorest

Table 3.1 Characteristics of commonly used satellite and their sensors

	Landsat	MOS	SPOT	IRS-1B	NOAA
Sensor	TM	MESSR	HRV/SX/P	LISS-II	VAHRR
Spectral Bands	7	4	3/1	4	3
Orbit Type	Sun Syn.	Sun Syn.	Sun Syn.	Sun Syn.	Sun Syn.
Inclination	98.25	99	98.70	98.70	98.80
Nominal Altitude	705km	909km	832km	832km	854km
Swath Width	185km	100km	60km	60km	3000km
Recurrent Period	16 days	17 days	3-4 days	22 days	every day
Ground Resolution	30m	50m	20m/10m	34 m	1.1km
Quantization Level	8 bit	6 bit	8 bit	8 bit	10 bit

quantization level. Different sensors have their own merits and demerits. SPOT panchromatic (P) mode has the best surface resolution but information contained only in a single band.

Landsat Multispectral Scanner (MSS) was the principal sensor of the Landsat 1,2, and 3. The scanning was accomplished by a mechanical scanning device

that acquire the data by scanning the earth surface in strips normal to the satellite motion. Six lines are scanned at a time by an oscillating mirror and the reflected energy is directed to 24 detectors represented four wavelength bands of the sensor. These incoming energy illuminates the detectors and produce continuously varying electrical signal corresponding to the energy received along the scanned line. The width of the each scanned line correspond to 79 meters on the ground. The effective pixel size on the ground is 79x79 meters. The energy that received at the detectors are converted into a digital value with respect to the electrical intensities that produce. This faster A/D transformation produce the nominal ground spacing of 56 meters betw2een readings. Because of this time difference that image produce a 56x79 meter image array, however the brightness values for these pixels are actually derived from 79x79 meter ground resolution cell. Characteristics of MSS sensors are summarized and shown in Table 3.2.

Table 3.2 Characteristics of the Landsat MSS sensor

Band Name	Spectral Region	Application
Band 4	0.5 - 0.6 μm	Coastal environment studies
Band 5	0.6 - 0.7 μm	Rock soil discrimination.
Band 6	0.7 - 0.8 μm	Turbidity of shallow waters
Band 7	0.8 - 1.1 μm	Discrimination of plant species

The Thematic Mapper (TM) of the Landsat series could be the most popular and served sensor for the remote sensing society. This is an enhanced version of the MSS sensor in spectral, radiometric and spatial resolution. The data acquisition is different from that of MSS as the TM sensor acquire the data in both directions. Also, within one scan line sixteen lines are swept simultaneously giving faster scanning time for better ground resolution.

Geometrically TM data are collected from 30x30 ground spacing, and 120x120 meter spacing for the thermal band. Radiometrically, the TM performs its analog to digital conversion over a quantization range of 255 digital numbers. This correspond to fourfold increase in the gray scale used by the MSS scanner. This finer radiometric resolution permits to observe smaller changes in the spectral magnitudes of ground features. The spectral characteristics and major fields of application of the TM data are given in Table 3.3.

Table 3.3 Spectral Characteristics of Landsat TM sensor

Band Name	Spectral Range	Major Field of Application
Band 1	0.42 - 0.52 μm	Coastal water mapping. Soil vegetation discrimination
Band 2	0.52 - 0.60 μm	Vegetation discrimination, and vigor assessment
Band 3	0.63 - 0.69 μm	Plant species differentiation, cultural feature identification
Band 4	0.76 - 0.90 μm	For vegetation type, vigor, biomass, estimation and water body delineate
Band 5	1.55 - 1.75 μm	Moisture and deficiencies identification, snow and cloud mapping
Band 6	10.4 - 12.5 μm	Thermal mapping, vegetation stress, moisture discrimination
Band 7	2.08 - 2.35 μm	Discrimination of mineral and rock types. Moisture in vegetation

The Indian Remote Sensing Satellites were launched in 1988 and 1991 respectively, They have two sensors, namely Linear Image Self Scanner I and II (LISS-I and LISS-II). The resolution of LISS_I is 72.5 meters and LISS-II got a resolution of 36.25 meters on the ground. Both of these sensors are

operated in four bands similar to that of Landsat MSS. Special characteristics of the sensor is shown in Table 3.4.

Table 3.4 Spectral characteristics of LISS-II sensor

Band Name	Spectral Region	Application
Band 4	0.45 - 0.52 μm	Coastal environment studies
Band 5	0.52 - 0.59 μm	Rock soil discrimination. Turbidity and bathymetry of shallow waters
Band 6	0.62 - 0.68 μm	Discrimination of plant species
Band 7	0.77 - 0.86 μm	Delineation of water features

Marine Observation Satellites (MOS) launched by Japan consists of three observation equipment; Multispectral Electronic Self-Scanning Radiometer (MESSR), Visible and Thermal Infrared Radiometer (VTIR), and Microwave Scanning Radiometer (MSR). The purpose of MESSR is to make obser4veation on sea and land surface, VTIR is for sea temperature measurements and MSR for observe the water vapor content, ice and snow distribution. Given resolution and spectral nature of the observation, the MESSR is the one which is suitable for land cover observation. MESSR sensor is designed to observe the earth surface in four spectral bands, Table in the visible and near-infrared regions. This employs an electronic scanning type radiometer, embodies charged coupled devices (CCD) for the detector. A CCD is a microelectronics silicon chip, a solid state sensor that detect light. When light strike the CCD silicon surface, electronic charge are produced, with the magnitude of the charge being proportional to the light intensity of the exposure time. Each CCD has 2048 photoelectric conversion elements in order to obtain 50 meter ground resolution. The image signal having been converted to an electrical signal by a CCD is fed to the signal processor where A/D conversion. The output digital values are quantized into 64 gray levels or 8 bits.

Table 3.5 Spectral characteristics of MESSR sensor

Band Name	Spectral Region	Application
Band 1	0.51 - 0.59 μm	Water quality in coastal area, plant distribution and volcanic ash mapping
Band 2	0.61 - 0.69 μm	Geological structure, Plant distribution, water quality of coastal areas and lakes
Band 3	0.72 - 0.80 μm	Surface water, plant species distribution, geological structures
Band 4	0.80 - 1.10 μm	Surface water, floods, vegetation, snow, ice mapping

SPOT sensor system has the finest resolution as at today. SPOT satellites are housed with tow identical High Resolution Visible (HRV) sensor systems operated in two modes; 10 meter resolution panchromatic mode in the 0.51 to 0.73 μm spectral region, and 20 meter resolution multispectral mode over the 0.50 to 0.89 μm spectral range. The system employs a push-broom scanning system with a linear array of CCDs arranged side-by-side along the line perpendicular to the satellite orbit track. A line of image data is obtained by sampling the response of the detectors along the array and successive lines of coverage are obtained by repeated sampling along the array as satellite moves over the earth. The CCD array of HRY consists of four sub-arrays, one for each band in the multispectral mode with 3000 elements for each of these. In panchromatic mode there are 6000 CCD elements. The energy observe at CCD are converted into digital with effective range of 255. The difference of this satellite from the others are its capability to observe the earth in oblique mode. With ground command the sensor can observe 27 degrees into its left or right facilitating higher repetitive coverage, and stereoscopic viewing in a given location. HRV sensor characteristics are tabulated in Table 3.6.

Table 3.6 Spectral characteristics of HRV sensor

Band Name	Spectral Region	Application
Band 1	0.50 - 0.59 μm	Coastal environment studies
Band 2	0.61 - 0.68 μm	Rock soil discrimination. Turbidity and bathymetry of shallow waters
Band 3	0.79 - 0.89 μm	Discrimination of plant species

3.3 Data Acquisition and Handling

There are no satellite that produce data free of charge to the end user except the NOAA series where the ground resolution is poor for land management studies. All other satellite data have to be purchased from respective agencies or local distributing centers. General flow of the remote sensing system is thematically shown in Figure 3.3.

The satellite products are provide as photographs or digital data. Photographs are map products produced in standard map scales. This product is the cheapest, and does not require special equipment to use in studies. The potential of satellite data can not be utilized by obtaining photographs as they have undergone various processing levels before reach the end user. Further they will not relay any information about the spectral response of ground features in the spectral bands in the satellites except by the colors in the film product. The advantage of multispectral observation will be lost in obtaining photographs as the possibility of band combination can not be achieved. Further, the analog nature will prohibit direct use of the information with other information.

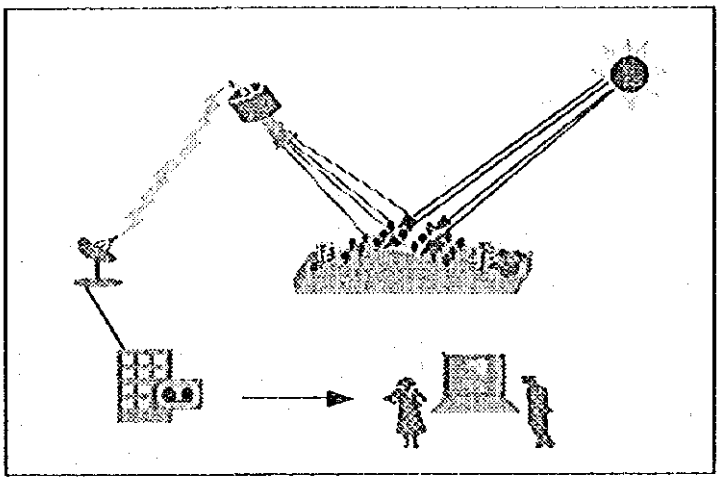

Figure 3.3 General flow of the remote sensing system

Digital products are relatively expensive than the analog products, but facilitate computer handling for information extraction. Ground receiving station carry out the required pre-processing for the user and it is requested to inform them with the processing level that is required by the user. There are advantages of purchasing digital data as it facilitate to discover the spectral response of ground features in the entire spectral ranges of the sensor. Handling of digital data requires special knowledge of computers, image processing and classification techniques. Also, suitable computer peripheral and software system is must for data handling. Figure 3.4 shows the working environment of the present work.

The energy that received by a sensor is transformed into a digital value, and transmitted to receiving stations. These digital values may differ due to different quantization levels of the sensors, and the prevailing condition of the atmosphere and position of the sun angle at the time of the ground pass of the satellite even for same surface cover on the surface. The radiation detected by a remote sensors travels through the atmosphere, and the atmospheric effect on the radiated energy varies with he locality and the prevailing weather conditions. The atmospheric attenuation is basically caused by the scattering and absorption.

It is important to note that a satellite data obtained for a particular area would give the status of the surface cover at the time of the observation. These observation may or may not give the current sate of the land use of the area.

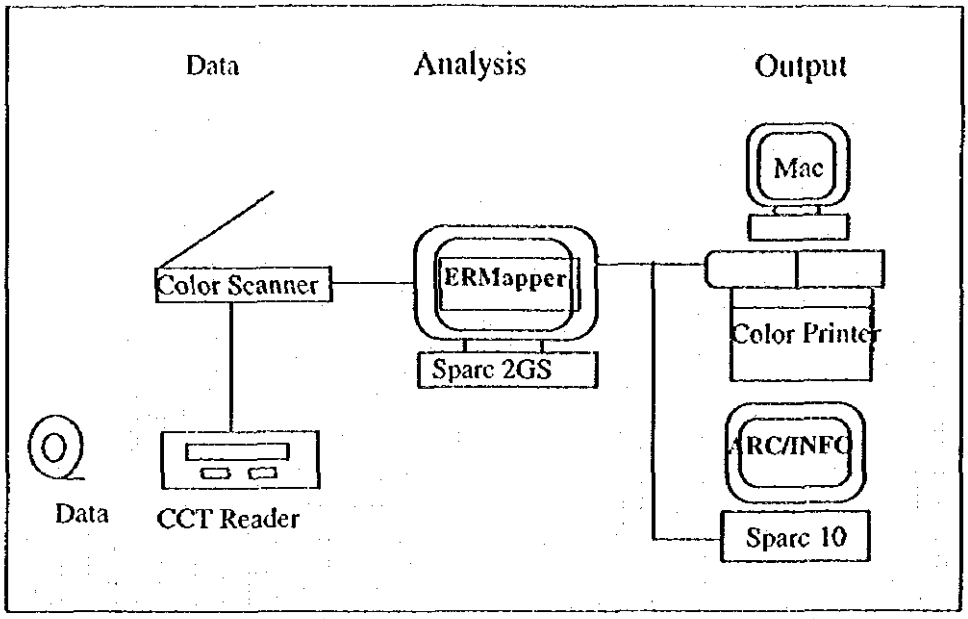

Figure 3.4 System configuration of the remote sensing analysis

3.4 Pre-processing of Satellite Data

When image data is recorded by sensor on satellite it can contain errors in geometry and in the measured brightness values of the pixel. Errors in image geometry can arise due to;

- rotation of the earth during image acquisition
- wide field of view of sensors
- curvature of the earth
- sensor non idealities
- variation in platform attitude, altitude and velocity
- panoramic effects related to image geometry

Radiometric distortion be either instrumentation effect or due to the transmission media, atmosphere.

3.4.1 Geometric Rectification

There are two technique that can be performed to correct various types of geometric distortions present in a digital image data. One is to model the nature and magnitude of the distortion mathematically, and use the mathematical models to correct. This one requires to characterize the distortion precisely. The other one, which is largely used defines a mathematical relationship between the addresses of image pixels with corresponding ground coordinates via maps or other coordinate information. The large popularity of this method is that the user can perform the correction without the precise understanding or modeling of distortion that are presented. In the latter one it is required to identify clearly identifiable features on the image and corresponding ones on maps. These well defined points both on the image and map are referred to as control points. This process can be enumerated in two steps; registering and rectification.

In the registering process control points are identified, their coordinate values are extracted and a relationship is established. In rectification stage, the established relationship is used to re-map the satellite data, pixel-by-pixel basis to the map projection.

Assuming that a position on the map can be denoted by (x,y), and the corresponding position on the image to be (u,v), these two coordinate system can be related through a pair of mapping functions f and g in the form;

$$u = f(x, y) \qquad \text{---------- (3.1)}$$

$$v = g(x, y) \qquad \text{---------- (3.2)}$$

Explicit form of the mapping function f and g are not known. Generally they are represented as a polynomial of first order or more complex higher order

polynomial. A simple first order polynomial, affine transformation can be accounted for most of the geometric perturbation in a satellite image. Using affine transformation above equation can be written as;

$$u = a_1 + a_2 x + a_3 y \qquad \text{---------- (3.3)}$$

$$v = b_1 + b_2 x + b_3 y \qquad \text{---------- (3.4)}$$

Theoretically, three control points will sufficient to solve the above equations for mapping coefficients. In practice however, it is not possible to choose control points without error, therefore many control points will be selected and least square technique is used to estimate the mapping coefficients. Selecting m number of points, the two residual sum of error can be represented as below;

$$\sum (u_i - (a_1 + a_2 x_i + a_3 y_i))^2 \quad i = 1 \ldots\ldots m \qquad \text{------- (3.5)}$$

$$\sum (v_i - (b_1 + b_2 x_i + b_3 y_i))^2 \quad i = 1 \ldots\ldots m \qquad \text{------- (3.6)}$$

Equation 3.5 and 3.6 are differentiated with respect to six unknowns, and the resulting equations are set to zero and solve simultaneously for coefficients.
Having defined the mapping polynomial it is required to find the points on the image that correspond to given location of the map. This process is rectification and involves some form of resampling. The image coordinate values estimated by mapping functions do not necessarily occur at the coordinate of original pixels on an image. Therefore, a procedure has to be formulated to estimate the spectral values of the pixels in the new image resulting after transformation from the original image. Most often used resampling methods are nearest neighbor, bi-linear and cubic convolution.
Nearest neighbor is the fastest method among these. This simply chooses the radiance value of the pixel that has its center nearest to the estimated image coordinate. The intensity (I) of the output pixel at (x,y) receives the intensity of the pixel (u,v) which is closest to the estimated position on the image.

$$I(x, y) = I(u, v) \qquad \text{------- (3.7)}$$

The bi-linear interpolation technique uses four neighboring pixels to estimate the intensity of the output pixel.

$$I(x, y) = a_{11} I(u, v) + a_{12} I(u, v+1) + a_{13} I(u+1, v) + a_{14} I(u+1, v+1) \quad \text{---- (3.8)}$$

where a_{11} ... a_{14} are coefficient and need to estimate using four radiance values. The cubic convolution uses sixteen points to estimate the intensity of the position of interest.

$$I(x, y) = a_{mn} I(u+m, v+n) \quad \text{where } -1 \le m, n \le 2-1 \qquad \text{------- (3.9)}$$

The nearest neighbor method the original intensities with half a pixel positioning error, while other two method will create new spectral radiance values.

3.4.2 Radiometric Distortion and Correction

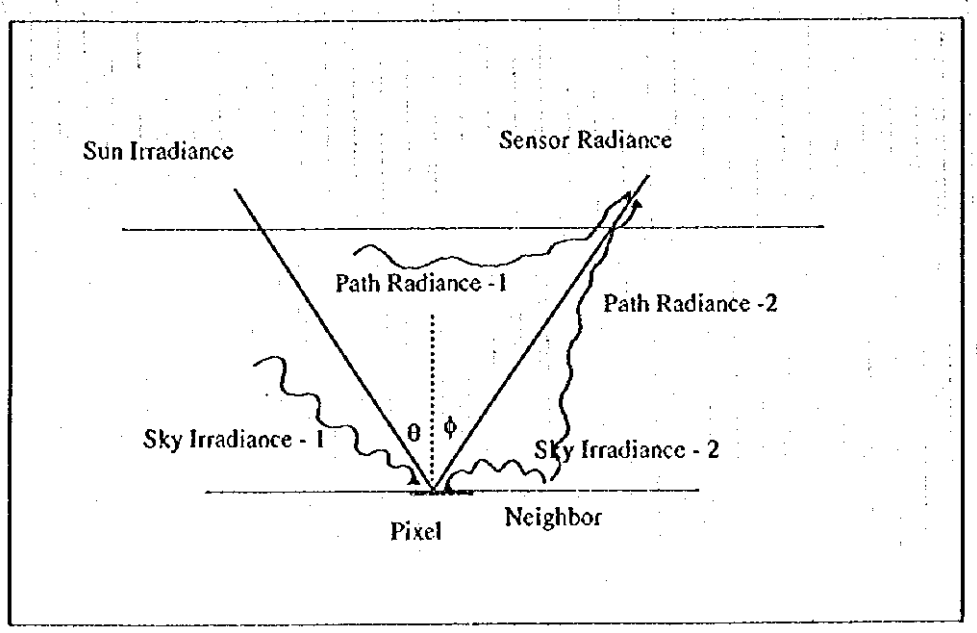

Figure 3.5 Energy interaction with earth surface

Effect of atmosphere and the surrounding has considerable amount of influence on the spectral radiance that receives at the sensor. Considered the atmosphere is not present, the energy that incident on a pixel from the sun is clearly defined and the radiance at the sensor is a function of spectral characteristics of the pixel that is observed.

Suppose there is no atmosphere then the solar spectral radiance at the earth can be calculated in a given range of wavelength as follows;

$$E_{os} = \int_{\lambda 1}^{\lambda 2} E_{\lambda} \cos\theta d\lambda \qquad \text{------- (3.10)}$$

E_λ is the spectral irradiance at the earth surface, θ is the solar zenith angle. E_{os} corresponds to the irradiance between wavelength λ_1 and λ_2. In remote sensing the wave bands are narrow enough to assume

$$E_{os} = E_{\Delta\lambda} \cos\theta \Delta\lambda \qquad \text{------- (3.11)}$$

where $E_{\Delta\lambda}$ is the average spectral irradiance in the band $\Delta\lambda$.

Suppose the surface reflectance is ρ and the surface is diffuse then the radiance that is available at the sensor will become

$$L = E_{\Delta\lambda} \cos\theta \Delta\lambda \rho / \Pi \qquad \text{------- (3.12)}$$

L is the incoming radiance at the sensor, it is possible to calculate the digital value that is correspond using detector response.

$$L = Ck + L_{\min} \qquad \text{------- (3.13)}$$

where $k = (L_{\max} - L_{\min}) / C_{\max}$ in which Lmax and Lmin are the maximum and the minimum measurable radiance of the sensor. These are usually available for the manufacturer and depend on the sensor system.

The above is a discussion of an ideal situation where the atmospheric interaction has been ignored. In reality there are certain interactions that should be considered during the energy travel from the sun and back to the sensor after interaction with the earth surface. The energy undergoes scattering and absorption during its pass through the media and the order of these perturbations are time and location dependent.

The absorption reduces the amount of energy that received at the sensor and at the target. The scattering process introduces additional component to the sensor radiance scattered from atmosphere itself. Further, neighboring pixel scattering would contribute to the target energy due to atmosphere. If we consider theses additional energy receives at the earth become

$$E_{os} = E_{\Delta\lambda} T_{\theta} \cos\theta \Delta\lambda + E_d \qquad \text{------- (3.14)}$$

T_θ is the transmittance and E_d is the diffuse sky radiance at the target. Then global irradiance become

$$L = \frac{\rho}{\Pi} \{ E_{\Delta\lambda} T_{\theta} \cos\theta \Delta\lambda + E_d \} \qquad \text{------- (3.15)}$$

The total radiance at the sensor become

$$L = \frac{\rho}{\Pi} \{ E_{\Delta\lambda} T_{\theta} \cos\theta \Delta\lambda + E_d \} + L_p \qquad \text{------- (3.16)}$$

To correct the atmospheric effect it is required to model the each scattering and absorption process using data obtained at the time of satellite pass. Generally there are no reliable data for model analysis of atmospheric correction. Most application that need to correct for atmospheric distortion uses graphical models for compensation for perturbations. Also, use of band ratios are said to be compensate for atmospheric differences for some extent.

Above discussion was based on considering the earth is a flat surface. In reality the undulation nature of the surface contribute differently to the

incoming solar radiation due to incident angle of the solar energy. This make the analysis difficult in hilly areas.

3.5 Outline of Image Analysis

The digital satellite data analysis can be addressed in two themes; visual interpretation and digital classification. As with photographic products digital data can be printed in hard copy with image enhancement techniques to improve the quality and requirements of the work. This will give the layman to visually identify features by investigating color, texture and homogeneity. In contrast to visual interpretation, satellite data can be classified using digital classification methods resulting thematic maps. This procedure involves specialized hands and high computer processing time, but process data can be treated easily for map generation in different scales and integration with other digital products for multi-disciplinary studies.

If not transformed the digital values of satellite observation for respective ground irradiance with rigorous computations they can not be taken as absolute reflectance of a for particular surface cover. The computations for this conversion involves supplementary data pertaining to atmosphere, sun position and satellite position at the time of the observation.

The complex mathematical computation could be avoided in classification digital remote sensing data if a relationship could be established between the ground features and the corresponding digital data. This is the most popular technique used in digital data classification. The general statistical classification techniques are summarized and shown in Figure 3.6.

The process can be break into two major parts; *Supervised Classification* and *Unsupervised Classification*. The unsupervised classification is a result of grouping satellite data itself for the natural groups within the observation, mathematically. This may or may not correspond to interested land cover classes. In supervised classification reference information for interested land

cover classes are collected at the time of the satellite pass. These information are compared with corresponding satellite observations in establishing mathematical or statistical relationships. Consequently, these relationships are used to classify the whole data set to the pre-selected land cover classes. The reliability of the final thematic maps are largely depend on the accuracy and the reliability of the reference information.

A combination of these two, referred to as Hybrid method in some literature is becoming popular as it consider the possible groups within a satellite data set before correlating with reference information.

The above methods are the most commonly used classification techniques. In order to identify dynamics of vegetation and their changes use of vegetation index are popular using spectral properties.

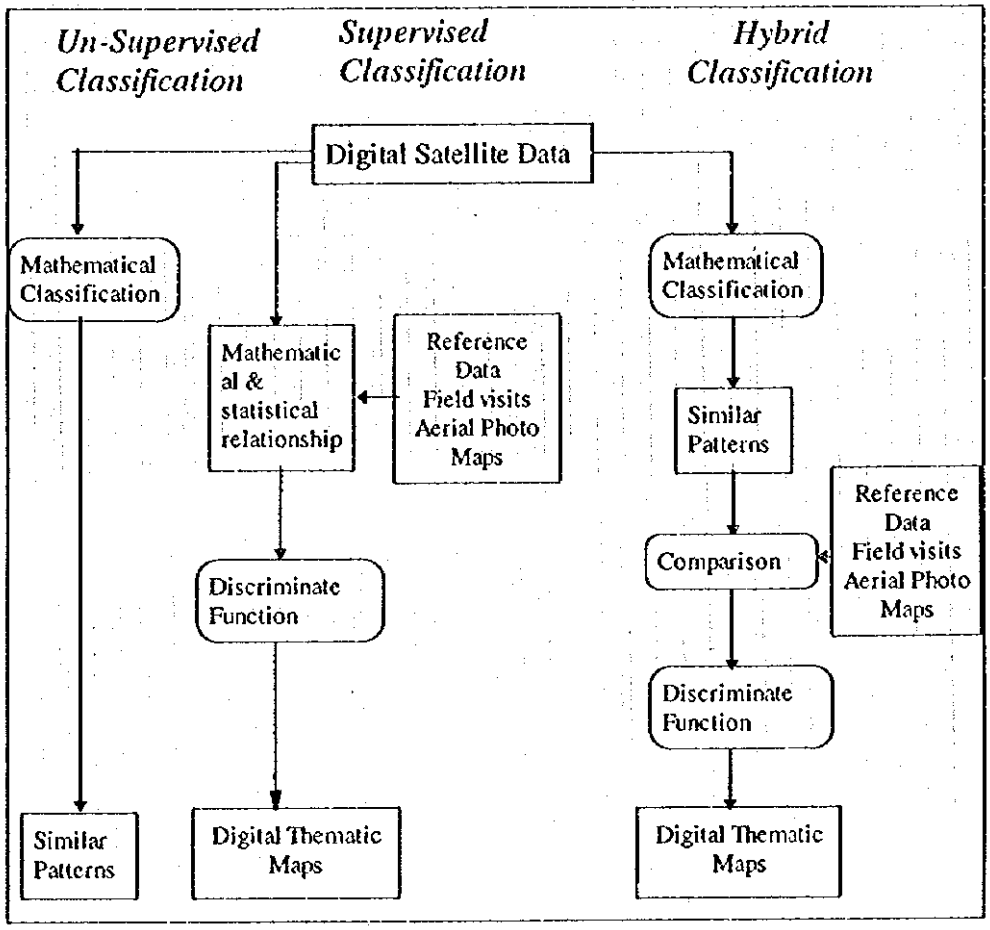

Figure 3.6 Outline of data classification

The cells in plant leaves are very effective scatters of light because of the high contrast in the index of refraction between the water-rich cell contents and the intercellular air spaces. Vegetation is very dark in the visible (400-700 nm) because of the high absorption of pigments which occur in leaves (chlorophyll, protochlorophyll, xanthophyll, etc.). There is a slight increase in reflectivity around 550 nm (visible green) because the pigments are least absorptive there. In the spectral range 700-1300 nm plants are very bright because this is a spectral no-man's land between the electronic transitions which provide absorption in the visible and molecular vibrations which absorb in longer wavelengths. There is no strong absorption in this spectral range, but the plant scatters strongly as mentioned above.

From 1300 nm to about 2500 nm vegetation is relatively dark, primarily because of the absorption by leaf water. Cellulose, lignin, and other plant materials also absorb in this spectral range. The most commonly used vegetation index is the Normalized Difference Vegetation Index (NDVI).

3.6 Remote Sensing Activities in Nepal

Remote sensing activities of Nepal has been started few years ago and there are some agencies that are active in this field. Also, this technology is used along with Geographical Information System (GIS) in most of the educational and other agencies. Some of the institutes that are using this technology are;

1. Forest Survey and Statistics Division
2. Mountain Environment and Natural Resources Information Services
3. Tribhuvan University - Central Department of Geography
4. Department of Mines and Geology
5 National Planning Council

National Remote Sensing Center was established in 1981 through a joint cooperation with the HMG/N and the USAID to conduct national level activities. It was the focal point for the remote sensing activities concerning natural resources evaluation and monitoring, well equipped with laboratory

facilities for photography, reprinting, reproduction with well trained manpower. During the period of 1985 to 1989 different international agencies; FAO, GTZ, JICA and UNDP involved in funding the center. During this period the center was very active. In 1989 the center was brought under the Forest Survey and Statistics Division as the remote sensing center. This change diverted the main objective of the national center to forestry need and it started to serve for forestry applications. By 1990 Finnish International Development Agency (FINIDA) funded the center for developing a Forest Resources Information System (FRIS). The initial funding was for four years, and later has been extended for another four years until 1999. The remote sensing and GIS facilities at this center are moderate as at today with trained personnel who are mainly engaged on preparation of data, some sort of GIS analysis, and remote sensing data interpretation. The center has Landsat Thematic Mapper Data covering whole Nepal taken in 1990 and 91. The centers has the authority to interact with outside agencies more freely as the semi-autonomous nature. The Mountain Environment and Natural Resources Information Services (MENRIS) was established in 1989 by International Center for Integrated Mountain Development (ICIMOD) program VI with a Technical Assistant Grant from the ADB, UNEP and GTZ. During its first phase, 1990 - 91 the center was engaged on establishing the MENRIS itself with proper staff and equipment, Training programs. The center is interested in database creation for the Hindu Kush-Himalayas, which is the target area of ICIMOD in development of an economically and environmentally sound mountain ecosystem and to improve the living standard of mountain population. The participating countries in this program are; Afghanistan, Bangladesh, Bhutan, China, India, Myanmar, Pakistan and Nepal.

MENRIS is active in GIS field by conducting training programs, creating a database, conducting collaborative studies with interested participating countries. The center is equipped with hardware and software for GIS data creation, analysis and presentation. Remote sensing is not active as GIS, and it is hoped that the center will take an active roll in this field with their new remote sensing specialist. In summary, the center is acting as the database manager, training center, and supervising agency in GIS for participating countries. In time to come it will create a similar environment for the remote sensing as far as the sponsor agencies are there. For details of system, data and services see Appendix 2-1.

Located in the Department of Geography in the Tribhuvan University it is aimed at introducing the GIS technology to the young graduates who are going to take an active roll in developing Nepal. The GIS facilities are donated by the ICIMOD under the funding of UNEP and ADB, and the GIS technology been introduced since 1994. Though the center is in its early stages the department already started GIS course works for final year geography students. It is said that the number of students who wants to take up the course exceeds the facilities in the department. Further, the department has started GIS training course for other government and non-government agencies. Two courses per year, in July and in December are conducted charging 25,000 Rs. as course fee. At present the department is preparing elevation database for entire Nepal by digitizing one inch topographical maps produced in 1962. This is a collaborative work with MENRIS, and Tribhuvan University is aiming to finish 200 topographical sheet within few months time. For course details and system configuration see the Appendix 2-1.

In the Department of Mines and Geology Remote Sensing lab was established in 1992 to extend this technology to geological and geomorphological mapping. Initial grant was provided by Germany with project duration for two years. No remote sensing equipment are available here. The required satellite pictures (analog form) are purchased from India or Thailand. These satellite pictures are used with aerial photographs and field verification for geological mapping.

A UNDP project was started in 1988 to improve the planning capacity, as well as serve as a integration body in the national level in the National Planning Council. Also, in 1992 a GIS project was initiated running for 30 months. This program was responsible for maintaining an information system for planning purposes of 24 districts of Nepal

As discussed in foregoing section these technologies are appearing in Nepal though it is limited to few agencies. Awareness of the technology among administrators and technical staff is acceptable. It is observed that the barrier for the expansion of GIS and remote sensing technologies are the initial cost of equipment, need of specialized man power and maintenance. Further, lack of proper integration of work in country level was observed. In some of the occasions, technologies have been started with the influence of foreign projects and the system are idling after completion of these projects. This

could be due to lack of the interest at managerial level, scarcity of funds, lack of demand from other agencies and poor coordination in country level. At present the most active agencies in data preparation of GIS are ICIMOD and Tribhuvan University, whereas in remote sensing the Forest Survey and Statistics Division is taking a leading role with specific interests. Also, it was said some NGO who are working on rural development are looking for GIS technology. It could be said that GIS is highly admired technology at the moment, and most of the agencies are working towards a common goal, creating a database. Within few years more data will be available, in different scales if the GIS specialists in Nepal keep their interest in this field, and the sponsor agencies continue their interest in developing databases for comprehensive studies. Transition of GIS database creation to productive analysis may take some more time as the data as at today may not be suitable for carry out scientific work for specific need. Further, object oriented analysis can not be performed without properly developed spatial database.

CHAPTER 4

DESCRIPTION OF THE STUDY AREA AND DATA ACQUISITION

CHAPTER 4 DESCRIPTION OF THE STUDY AREA AND DATA ACQUISITION

4.1 Outline of the Study Area

General model for describing the basic landscape elements of the Nepal Himalaya is shown in Figure 4.1. The maximum altitude exceeds 8000 meters and the maximum depth of sediment reaches more than 5000 meters below the sea level. This dramatic deposition and elevation difference in between rather narrow north-south extent reflects the enormous crustal movement that has occurred and is occurring at present. There are three main tectonic discontinuities that are responsible for deformation and elevating the mountain range; Main Central Trust Zone (MCT), the Main Boundary Fault (MBF), and the Main Frontal Trust (MFT). These trust are parallel to the entire Himalayan system. The region is subdivided or identified according to their physical, or ecological or physiographic nature by different authors Table 4.1.

The four northern units Tibetan Plateau, Tibetan Marginal Range, Greater Himalaya and the Inner Himalaya are grouped as High Mountain. This area extends beyond 4000 meters, and above the montane forest belt. The higher north facing slopes are semi arid or arid because of high altitude rain-shadow effect. The south slopes intercept the summer monsoon, and precipitation decreases with increasing altitude.

Middle Mountain lies south of High Mountain, and this area comprises much of the population of the Himalaya. The northern section runs below 4000meter montane forest cover and in south adjoining agricultural lands.

The Mahabharat Lekh and the Siwalik constitute the Lesser Himalaya bounded against the Ganges plain, Terai. The MFT has produced enough deformation to rose this area over Terai plain. Mahabharat Lekh and the Siwalik are composed of young tertiary strata and contains some of the most easily erodible lithologies including unconsolidated sand and gravel. The Siwalik stand over the Ganges plain with an altitude ranging from 200 to 1500 meters.

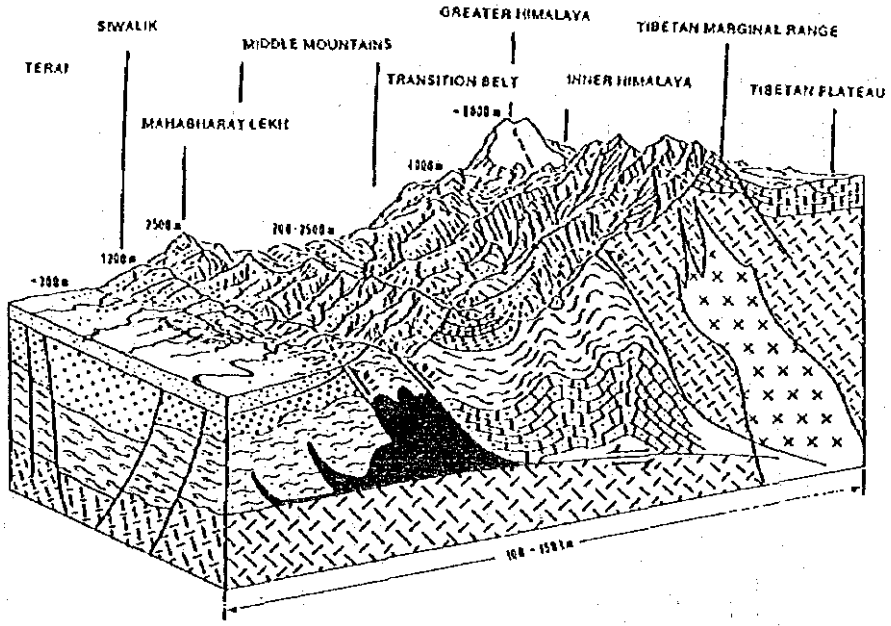

	Litho-tectonic units	Rock type
	Quaternary	Alluvial sediments
	Upper	
	Middle - Siwalik	"Molasse" sandstone & shale
	Lower	
	Paleozoic and younger sediments of the lesser Himalaya	Schist & Limestone
	Paleozoic and younger sediments of the Higher Himalaya	Limestone & Marl
	Upper Precambrian and Lower Paleozoic sediments	Phyllite & Quartzite
	Lower Precambrian crystalline basement	Gneiss & Migmatite
	Tertiary Leucogranite	Tourmaline Granite
MFT	Main Frontal Thrust	
MBT	Main Boundary Fault	
MCT	Main Central Thrust	

RESEARCH REPORT ON THE INVESTIGATION OF LANDSLIDE AND SOIL EROSION IN NEPAL USING REMOTE SENSING TECHNOLOGY

Figure 4.1 Geography of Himaraya

JAPAN INTERNATIONAL COOPERATION AGENCY

Table 4.1 Physical division of Himalayan landscape (after Ivans, 1989)

Geographic Region (native term)	Hagan Physical feature	Gurung Physical feature	FAO/HMG/UNDP Ecological zone	LRMP physiographic zone
Mountain (Himal)	Tibetan Marginal Mountain	Border Range		
	Inner Himalaya	Trans-Himalyan Valleys	High Himalaya	High Himalaya
	Himalaya (Himal)	Himalaya	Transition zone	High Mountain
Hills (Pahar)		Temperate (lekh) Sub tropical (Pahar)		
	Midlands			
	Mahabharat Lekh	Mahabharat Lekh Inner Terai Chrure range	Middle Mountain	Middle Mountain
Plain (Terai)	Siwalik zone		Siwalik	Siwalik
	Terai	Terai	Terai	Terai
Source	Hagan (1960)	Gurung (1971)	Nelson (1980)	HMG (1986)

Ratu watershed, which is situated in the Siwalik was selected for the present study, Figure 4.2. Ratu river originates from a Churiya hill in central Nepal at an altitude of 700 meters and drains into Terai region, few kilometers north of Janakpur. The watershed lies west of Kamala river and south of Sun Koshi. Ratu river crosses the East-West highway around 86E and 27N. River runs dry during the winter and transport sediments during the rainy season with the high water flow. The sediment unloading capacity said to be very high during a heavy rainfall or continuous rainfall during the monsoon. The riverbed gradient is very gentle, and the average bed slope from the Highway to its origin is only 1%. This indicate that the sediment transporting capacity may not be attained without considerable amount of precipitation.

As the watershed is belonged to the Siwalik or the Churiya Hills, the rocks are represented by soft and loose sandstone, mudstones, and conglomerate. The

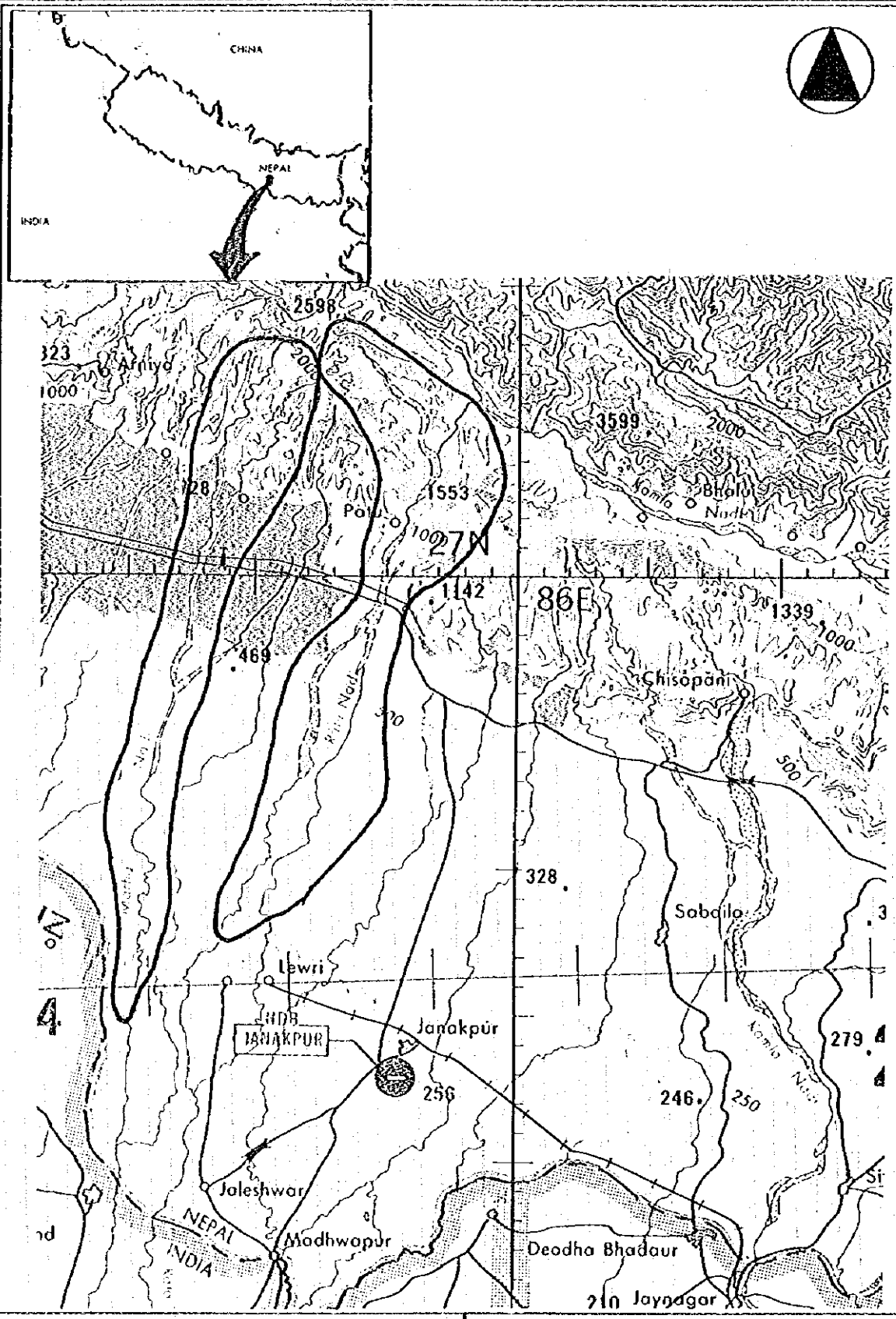

RESEARCH REPORT ON THE INVESTIGATION OF LANDSLIDE AND SOIL EROSION IN NEPAL USING REMOTE SENSING TECHNOLOGY

Figure 4.2 Study area

JAPAN INTERNATIONAL COOPERATION AGENCY

topography is predominantly steep except in the lower part of the watershed where it is possible to observe some gentle slope hills. About 70% of the watershed area is covered by forest with varying cover densities. *Shorea Robusta* , locally called *Sal* is the major species that found in the area. Over the upper reach, it could be said that the crown closure is above 75%, according to the 1992 aerial photo interpretation, Figure 4.3. Remaining land could be grouped into two; crop lands and barren land. It is said that the depth of the soil layer is less than 20cm in the Churiya Hills, probably same in this watershed. This soil layer is very fragile as very extreme erosion hazard and poor regeneration potential.

4.2 Acquisition of Remote Sensing Data

Consideration was made to two aspect of the present study in acquiring remote sensing data. One objective of the study is to estimate the planform change of Ratu river and impact on the floodplain. In this aspect, it was decided to obtain satellite remote sensing data over a long time span giving the opportunity to extract information of physical changes that have been taken place in the watershed, and in the floodplain. The other purpose of the present study is to establish a soil production model with limited data that is available for the present study area and for most of the watersheds in the Siwalik. As there was no runoff gauges within this watershed, the validity could only be carried out by comparing changes of deposit during a given time span. Further, field work was requested for identify the physical nature of the soil erosion, its transport and sedimentation.

Therefore, satellite dataset covering a major flood event was considered to estimate the area of sedimentation. The most recent flood event, 1993 July was selected for this as this could give the opportunity to collect the information on the extent and nature of the flood and consequences by visiting the field where no other means of information can be obtainable.

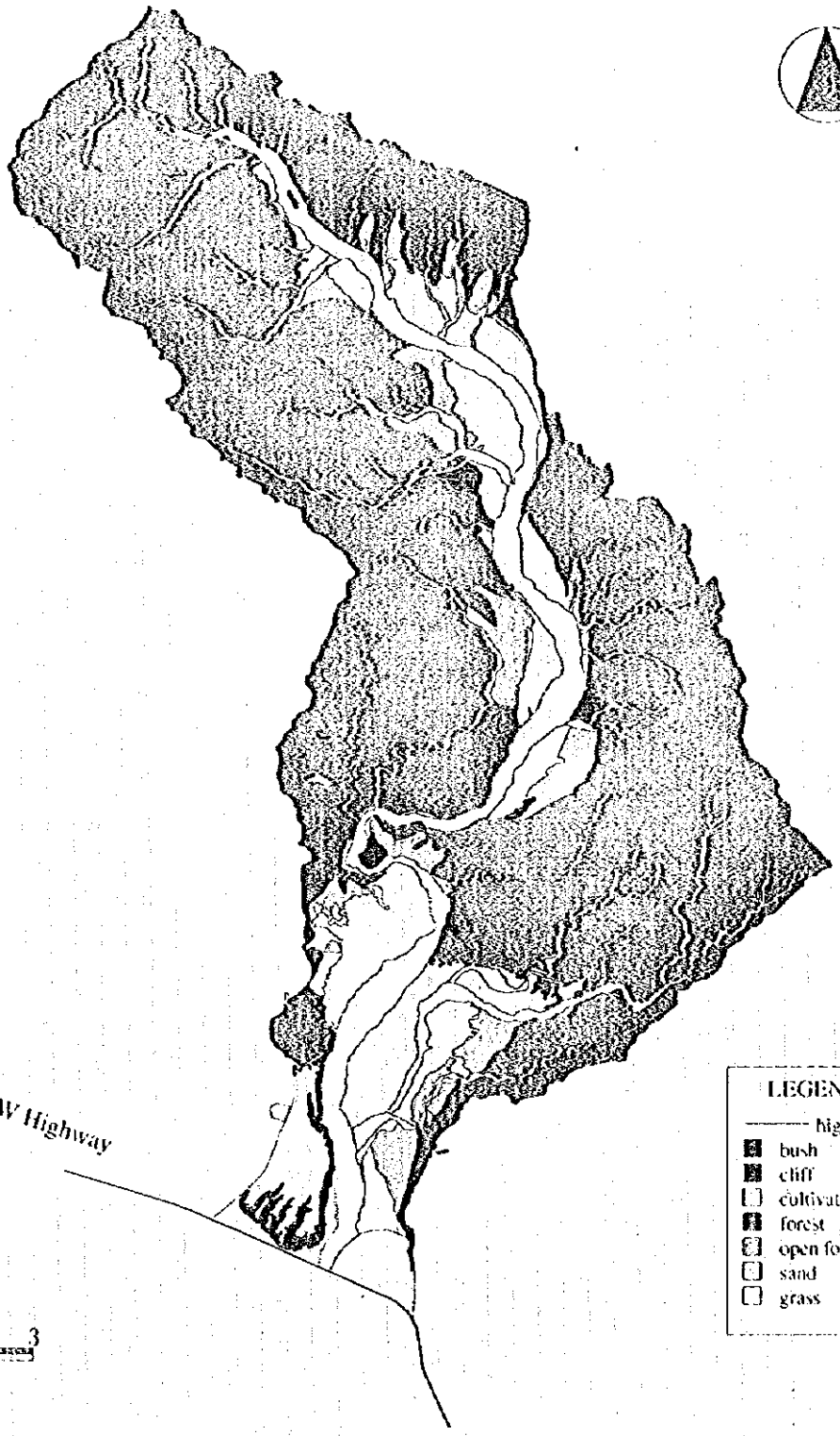

RESEARCH REPORT ON THE INVESTIGATION OF LANDSLIDE AND SOIL EROSION IN NEPAL USING REMOTE SENSING TECHNOLOGY

Figure 4.3
Land cover map of the study area

JAPAN INTERNATIONAL COOPERATION AGENCY

Satellite remote sensing data are available form the first launch of Landsat satellite series. These data are supposed to available from 1973 observed by MSS scanner of Landsat systems. For recent dates, specifically after 1990 there are different sensors like Landsat TM, SPOT, IRS, JERS could have covered the study area for the interested dates of the present work. Preference was given to Landsat series in selecting data as its availability for a long period.

As the initial step of data acquisition, information on the dataset available for each sensor from 1973 onwards were requested from data distribution centers here in Japan and Thailand. It was found that no data was available for the period 1980 to 1990 for this area. Also, the area was not observed, or no data with suitable cloud cover was present for the period May to November for any sensor from 1973 to 1995. This could be due to the fact that this period is belong to the monsoon rainfall season and there could be high cloud cover present over the study area. Considering the objectives of the project, major flood events and the budget allocated, the data shown in the Table was selected for the present study. Further, during the selection of data, special attention was given to choose data that are acquired in the same day of the year, or same season of the year to minimize irradiance variations on the surface due to positional differences of the sun. Information of the selected datasets on the position of the sun at the time of satellite pass are given in Table 4.2.

Table 4.2 Information on the satellite data obtained for the study

Sensor	Date	Sun Angle	Sun Azimuth	Processing Level
MSS	1973.03.14	Not Known	Not Known	Bulk
MSS	1977.03.20	Not Known	Not Known	Bulk
TM	1993 .03.16	47	127	Bulk
TM	1995 .03.22	46	122	Bulk
LISS-II	1994.11.15			Bulk
LISS-II	1995.03.15			Bulk

4.3 Ground Truth Data Collection

The best source of information of any phenomenon under consideration can be obtained only by examining it in the field. Further, for analysis of remote sensing data, availability of a set of reliable reference information is a pre-requisite. This is because remote sensing data represent relative radiance of the area of observation and can not be converted to physical features of the area unless the relationship of relative radiance values with the physical features on the ground is not formed. Therefore, it was decided to carry out ground survey for collection of information on the current state of the Ratu watershed, and to identify the nature and process of soil production and propagation through main stream to the flood plain in the Terai region. Collection of ground truth and field investigation carried out is enumerated below.

1. Acquisition of aerial photographs

Referring to the availability of satellite data and major flood events, requisition was made to the Topographical Survey Department of Nepal for aerial photographs. The study area has been covered by 1992 November aerial photographs in the scale of 1:40,000. As this coverage depicts the state of the watershed, and the area of sedimentation due to flood event of 1992 June, photographs that cover the Ratu watershed were obtained for the analysis.

Further, a set of photographs in a similar scale obtained in 1979 was obtained for comparison with satellite data for establishing spectral properties of satellite data of interested cover classes.

2. Collection of Helicopter photographs

The aerial photographs are in small scale and taken in the wet season limiting the comparison with satellite data in estimating vegetation growth and vigor using NDVI (Normalized Difference Vegetation Index). Therefore, it was

decide to photograph the Ratu watershed using a helicopter. A normal camera that uses visible light with 50mm focal length was used to obtain vertical or near vertical photographs flying at an altitude of 1200 meters. OpeRaturs were taken care to keep the camera vertical for their extent on the shaking helicopter. Simultaneously, a camera with infrared filter was used to film the same location filmed by the normal camera to compare with the infrared spectral band of the satellite data. The route of the helicopter and the photographed location are shown in Figure 4.4. The accurate locations were identified by comparing small scale photographs with topographical maps.

3. Field survey information

Field visits were requested to survey some of the sub-streams of the Ratu river and observe the river bed for sediment formation, distribution and clues to differentiate the age of the depositions. Few river cross sections were requested, specifically in the upper stream and flood plain to evaluate the volume that has been deposited through different flood events. The results are further discussed in chapter 6.

4.4 Collection of other Conventional Data

In addition to satellite data the following data were collected for the present study.

Geological Maps	1:250,000
Geographical Maps	1:25,000
Climatic Records of Nepal	
Land Capability Maps	1:50,000
Land Utilization Maps	1:50,000
Land Form Maps	1:50,000

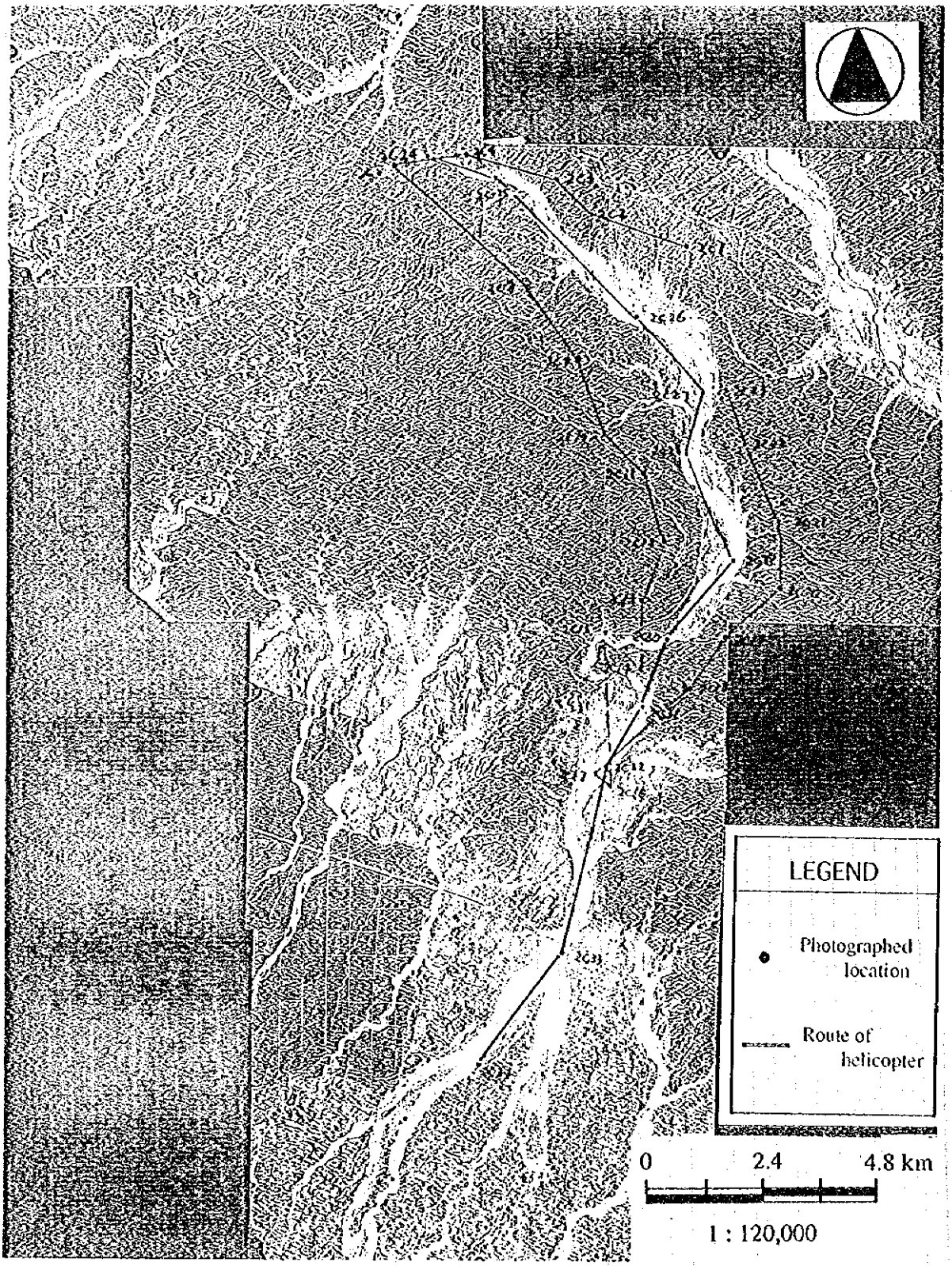

RESEARCH REPORT ON THE INVESTIGATION OF LANDSLIDE AND SOIL EROSION IN NEPAL USING REMOTE SENSING TECHNOLOGY	Figure 4.4 Helicopter route for photography
	JAPAN INTERNATIONAL COOPERATION AGENCY

CHAPTER 5

ANALYSIS METHOS AND DATABASE CREATION

CHAPTER 5 ANALYSIS METHOD AND GIS DATABASE CREATION

5.1 Method of the Analysis

As explained in earlier chapters, the rapid soil loss and sedimentation due to intensive rainfall can be considered as consequences of surface erosion induced by human intervention or natural phenomena. In order to verify these erodibility factors and to establish the mechanism of soil erosion and sedimentation in the Ratu watershed the analysis, was carried in the present study following themes;

- Sediment budget by field surveys
- Sediment deposition and planform changes of river channels by remote sensing
- Amount of soil yield (volume) by remote sensing and GIS technology
- Temporal analysis of volume of soil production and planform variations by remote sensing data

Here, the estimate of extents and its changes can be considered as a direct measurement from remote sensing data, and the accuracy is depend on the spatial resolution of the particular sensor. To evaluate the soil balance, which is a volumetric estimation requires not only the surface extent but also the depth of the deposition and rate of denudation. The depth has to be acquired from other methods. Deposition depth and the production rate can be obtained by direct investigation, or using indirect measurement that support the rate of denudation. The major items of the analysis procedure and their relation to data and observation are presented in Figure 5.1.

The field visit estimated sediment budget results were compared with satellite data estimates to evaluate the applicability of remote sensing and GIS technologies in soil erosion and sedimentation problem in the Ratu watershed.

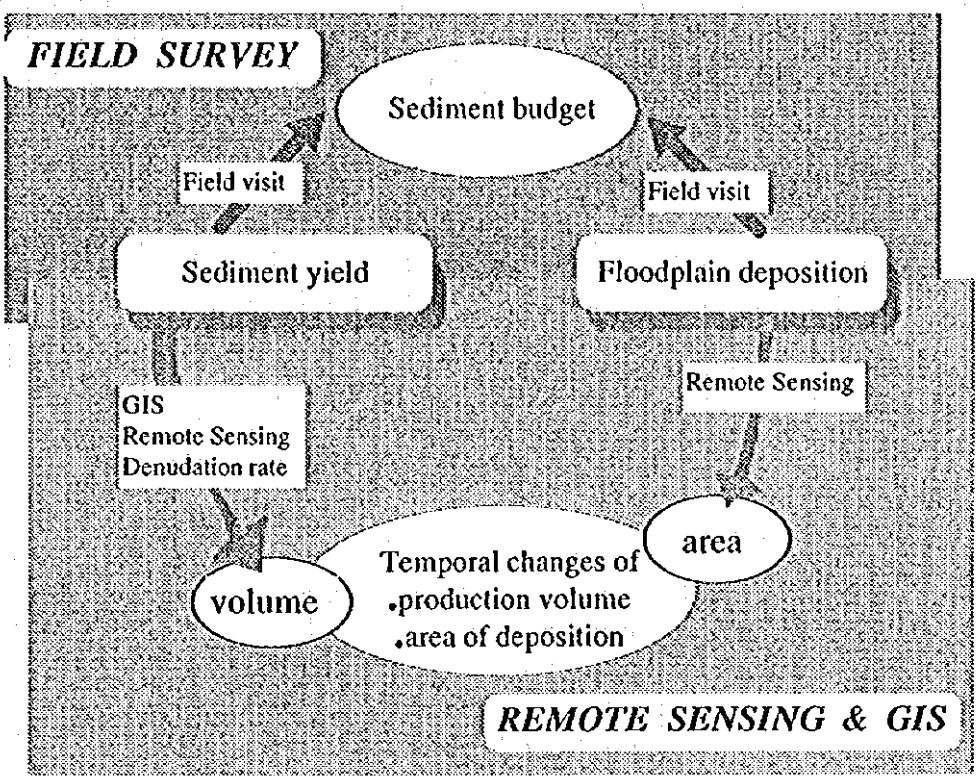

Figure 5.1 Main components of the data and analysis

5.2 Potential of a Geographic Information System (GIS)

Geographical Information System(GIS) is a computer assisted system for acquisition, storage, analysis and displaying of geographic data. Comprehensive disaster mitigation project requires handling of huge volumes of spatial data and extensive spatial analysis. With its inherent power of store, manage, manipulate and present spatial data, the GIS technology is increasingly preferred in natural disaster monitoring and mitigation projects. The performance of this technology has been appealing owing to the improved capabilities of computer hardware. The enormous amounts of spatial data such as maps and drawings to represent natural resources information and human activities such as topography, rivers, forest cover, landuse, houses, utility facilities can be efficiently input, stored and managed in an intelligent database. GIS can perform a variety of spatial operations such as polygon overlays, proximity analysis and surface modeling. Moreover, these operations can be performed at much better speeds and higher spatial accuracy that are not possible by conventional and manual methods. Such capabilities of GIS can be summarized as follows.

• Geographical data processing and visualization

Using GIS, geographical information which are collected in a variety of forms such as maps, drawings, documents, tabular sheets, photos, etc., are converted into digital form and stored in a computer database. These data are standardized geographically in terms of coordinate system, units, map projection and spatial accuracy prior to further processing and analysis. Once the information is captured into GIS, high quality thematic maps can be easily made based on user defined scale, color, symbol patterns, or visually presented on graphical display instead of hard copy outputs.

• Database management

GIS integrates tabular data and map data commonly in relational database providing two way interaction - map to table (query, information update) and table to map(query, update, presentation) . Information in the database can be shared efficiently among users and allows to avoid confusion by multiplexed information. National/local governments would receive a great deal of benefits from this capability especially in urban and regional planning and facility management.

• Spatial analysis

Spatial analysis is extensively used in many practical applications such as slope stability, environmental impact of road construction, etc. GIS stores the various types of spatial information of the study such as geology, soil type, basin boundaries, etc. as separate layers. There are different layers for different types of information which are represented by points, lines, and polygons. Given the problem, analysis can be carried out using the required thematic layers for the best or for the optimal solution. For example, it possible to calculate the areas of new sedimentation and the social impact after a flood event by overlaying the information layers such as rivers, household, land use before flood, and land cover after the flood event.

Other typical spatial analysis tools provided by GIS are spatial interpolation, topographic (surface) analysis, network analysis. A Computer Assisted Design (CAD) system, which is commonly used in architect and construction

firms, also has similar graphical data processing functions. The major difference in such capabilities between GIS and CAD is that the GIS can manipulate graphical data in connection with tabular data.

The data of GIS should be thought of as representing a model of the real world (eg. Bouillè 1978). They can be accessed, transformed, and manipulated interactively, and can serve as a test bed for studying environmental process or for analyzing the results of trends, or of anticipating the results of planning decisions. It is possible for planners and decision-makers to explore a range of possible scenarios and to obtain an idea of the consequences of a course of action before the mistakes have been irrecoverably made in the landscape itself (Burrough 1986).

5.3 Creation of Thematic Information

Spatial information that are required for the soil erosion estimation, river channel monitoring and defining the physical nature of the soil production, transport and sedimentation, was converted into digital form constructing a GIS database for the present work. For example, the surface information such as slope and aspect which are necessary to estimate the soil erosion potential was obtained by digitizing topographical maps of the area and creating a Digital Elevation Model (DEM). Land use of the watershed and the floodplain is indispensable information to compare with Vegetation Index derived from image processing of satellite data in order to recognize the degree of watershed degradation, denudation and estimate the social impact on a flood event. Base maps collected and general description of the database are listed in Table 5.1. These maps were digitized and a GIS database was created.

Feature attributes of each data are stored in the form of relational database as feature attribute table, where one record represents a series of attributes of one individual map feature.

Table 5.1 Incorporated information into the GIS database

BASEMAPS	TOPOGRAPHIC MAP	(1:50,000)
	TOPOGRAPHIC MAP	(1:25,000)
	LANDUSE MAP	(1:50,000)
DIGITIZED AREA	Sheet 72 E/15, E/16, F/13	(1:50,000)
COORDINATE SYSTEM		
	Universal Transverse Mercator, Zone 45	
DATA	Topographic Contour (100ft.)	:line
	Topographic Contour (20m.)	:line
	Geological Map	:polygon
	Road	:line
	River	:line
	Landuse	:polygon
	Land System	:polygon
	Land Capability	:polygon

5.4 Integration GIS and Remote Sensing Data

As it is explained in Chapter 3, the satellite data obtain from the receiving centers do not represent common geographic projection restricting comparison without rectification. The procured satellite data were brought in to a common map projection by constructing relational functions those relate satellite data projections with map projection. Rectification process was conducted as described in Chapter 3 using UTM projection as the objective reference system. First order transformation functions were established for all the datasets, and nearest neighbor resampling was used for re-mapping the satellite data into the UTM projection. TM data sets were rectified with less than 20m rms. error, for MSS the rms. was 25 and it was 22 for IRS data. As these data were rectified for same map projection that of GIS database it was possible to

compare, and use them to analysis with other conventional data for present objectives. The completed GIS database together with the rectified remote sensing data and the analysis procedure is shown in Figure 5.2.

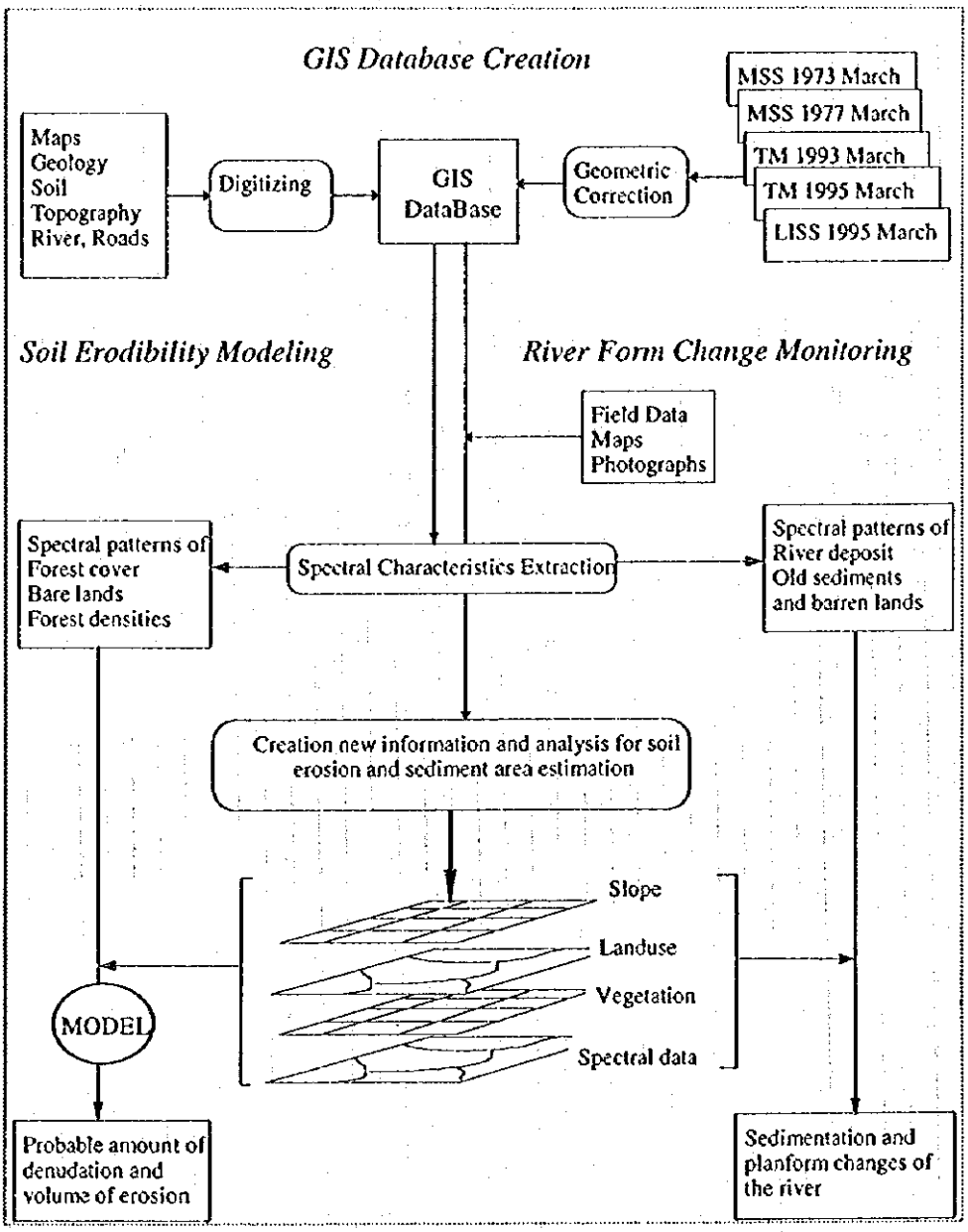

Figure 5.2 GIS oriented satellite data analysis procedure for study objectives

5.5 Derivation of Surface Parameters

The created database was further manipulated for creation of surface parameters that required for estimation of soil erosion productivity. The most related surface parameters with the productivity of surface erosion and slope failures are slope and surface facing. The south facing ridges are highly degraded than north facing ones. For calculation of slope or the maximum gradient of a point of interest and its look direction a DEM was using digitized topographical maps.

- Creation of DEM

Digital Elevation Model (DEM), a digital representation of the continuous variation of relief over space in a grid cell format, was created from contour line data. Considering the complexity of the geomorphology of the Ratu watershed and taking into account the scale of the base map, the digitizing accuracy it was decided to generate 10 meter grid interval for creation of DEM. Though there are several procedures to create DEM from vector type contour lines, linear interpolation method using TIN (Triangulated Irregular Network) was selected for this project, Figure 5.3.

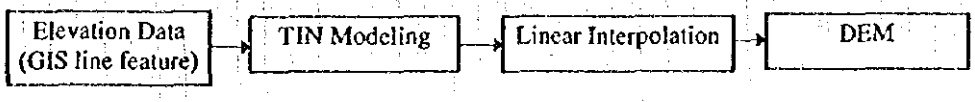

Figure 5.3 Creation of DEM from contour lines

TIN is a very efficient surface modeling technique. A TIN uses a sheet of continuous, connected triangular facets based on a Delaunay triangulation of irregularly spaced nodes or observation points as shown in the Figure 5.4. Unlike the altitude matrices, the TIN allows extra information to be gathered in areas of complex relief without the need for huge amounts of redundant data to be gathered from areas of simple relief. The data capture process for a TIN can specifically follow ridges, stream lines, and other important topological features(Burrough 1986).

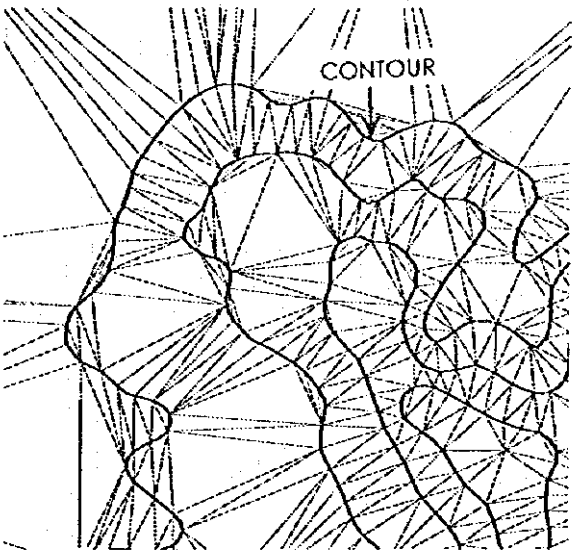

Figure 5.4 An example of a TIN structure

In linear interpolation based on TIN, the surface value to be interpolated is calculated based solely on the z values for the nodes of the triangle within which the point lies, Figure 5.5. The surface value is obtained by intersecting a vertical lines with the plane defined by the three nodes of the triangle. The generalized equation for linear interpolation of a point(x,y,z) in a triangle facet is:

$$Ax + By + Cz + D = 0$$

where A,B,C, and D are constants determined by the coordinates of the triangle's three nodes.

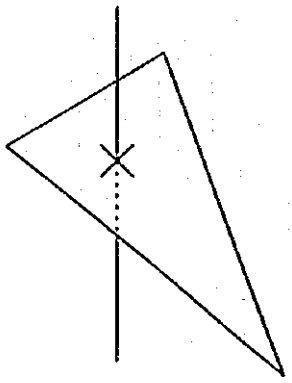

Figure 5.5 Triangle facet and grid point

• Slope and aspect calculation

Using DEM, slope angle and slope aspects were calculated using 3 x 3 kernel in Figure 5.6.

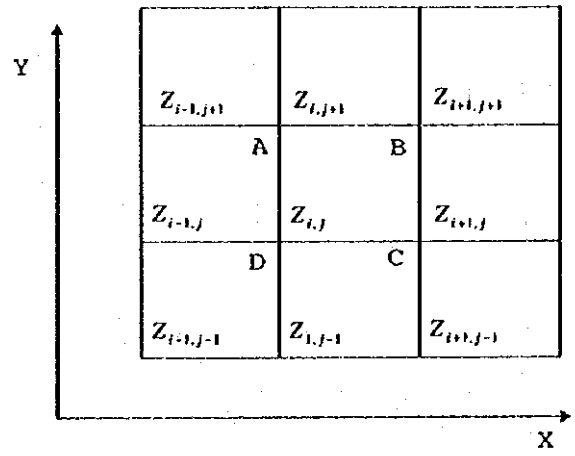

Figure 5.6 Kernel used for computing slope angle & aspects

Based on the kernel, slope angle and aspects were calculated using following formula;

Elevation increment in Eastward:

$$[\delta Z/\delta X]_{i,j} = \left[\left(Z_{i+1,j+1} + 2Z_{i+1,j} + Z_{i+1,j-1}\right) - \left(Z_{i-1,j+1} + 2Z_{i-1,j} + Z_{i-1,j-1}\right)\right] / 8\delta x$$

Elevation increment in Northward:

$$[\delta Z/\delta Y]_{i,j} = \left[\left(Z_{i+1,j+1} + 2Z_{i,j+1} + Z_{i-1,j+1}\right) - \left(Z_{i+1,j-1} + 2Z_{i,j-1} + Z_{i-1,j-1}\right)\right] / 8\delta y$$

Thus, Slope angle G can be represented as:

$$\tan G = \left[(\delta Z/\delta X)^2 + (\delta Z/\delta Y)^2\right]^{1/2}$$

also, aspect A can be defined as:

$$\tan A = \frac{-\delta Z/\delta Y}{\delta Z/\delta X}$$

$Z_{i,j}$: Elevation

$X_{i,j}, Y_{i,j}$: x,y coordinate

$\delta x, \delta y$: Cell interval

Mathematical concept of the above equation is described below;
Elevations of A,B,C & D in the figure can be interpolated as,

$$A = \frac{Z_{i-1,j+1} + Z_{i,j+1} + Z_{i-1,j} + Z_{i,j}}{4}$$

$$B = \frac{Z_{i,j+1} + Z_{i+1,j+1} + Z_{i,j} + Z_{i+1,j}}{4}$$

$$C = \frac{Z_{i-1,j} + Z_{i+1,j} + Z_{i,j-1} + Z_{i+1,j-1}}{4}$$

$$D = \frac{Z_{i,j} + Z_{i+1,j} + Z_{i,j-1} + Z_{i+1,j-1}}{4}$$

Elevation increment in eastward can be defined as;

$$\frac{\partial Z}{\partial X} = \frac{\left(\frac{B+C}{2} - \frac{A+D}{2}\right)}{\delta x}$$

Therefore,

$$\frac{\partial Z}{\partial X} = \frac{B + C - A - D}{2\delta x}$$

$$= \left(\begin{array}{l} Z_{i,j+1} + Z_{i+1,j+1} + Z_{i,j} + Z_{i,j+1} + Z_{i,j} + Z_{i,j+1} + Z_{i,j-1} + Z_{i+1,j-1} \\ \quad - Z_{i-1,j+1} - Z_{i,j+1} - Z_{i-1,j} - Z_{i,j} - Z_{i-1,j} - Z_{i,j} - Z_{i-1,j-1} - Z_{i,j-1} \end{array}\right) \Big/ 4 \cdot 2\delta x$$

$$= \frac{Z_{i+1,j+1} + 2Z_{i+1,j} + Z_{i+1,j-1} - Z_{i-1,j+1} - 2Z_{i-1,j} - Z_{i-1,j-1}}{8\delta x}$$

Thus, elevation increment in eastward is;

$$\left[\delta Z/\delta X\right]_{i,j} = \left[\left(Z_{i+1,j+1} + 2Z_{i+1,j} + Z_{i+1,j-1}\right) - \left(Z_{i-1,j+1} + 2Z_{i-1,j} + Z_{i-1,j-1}\right)\right] / 8\delta x$$

Also, elevation increment in northward is;

$$\left[\delta Z/\delta Y\right]_{i,j} = \left[\left(Z_{i+1,j+1} + 2Z_{i,j+1} + Z_{i-1,j+1}\right) - \left(Z_{i+1,j-1} + 2Z_{i,j-1} + Z_{i-1,j-1}\right)\right] / 8\delta y$$

CHAPTER 6

PHYSICAL MECHANISM OF SOIL PRODUCTION AND SOIL BALANCE OF RATU WATERSHED

CHAPTER 6 PHYSICAL MECHANISM OF SOIL PRODUCTION AND SOIL BALANCE IN RATU WATERSHED

6.1 Characteristics of Ratu Watershed

6.1.1 Geological and Morphological Characteristics of the Watershed.

Ratu River is situated about 8.0 kilometers South of Sindhulimadi, and flow in the direction of north-south from Siwalik Hills to the Terai region, and consequently drained into Bay of Bengal. The nature of Ratu is a typical to Siwalik Hills. This river has two features. The first is *wadji* that has not water stream except rainy season. The second is the capability of high debris production forming a wide flooding area.

To exploit the application of satellite remote sensing to identify the sediment yield and to develop a methodology to grasp the disaster condition of the Siwalik area the field work was concentrated over the whole watershed and the floodplain. The East-West Highway (hereinafter EWH) could be considered as the *standard* point of upper watershed and the floodplain.

Ratu river drains from its source to South-East and change its direction to Southward from the confluence point with Arne river, one of the sub-stream of Ratu river. For this reason, watershed of this river shows the combined shape of two rectangles. Drainage pattern is dendritic and parallel, Figure 6.1. Length of the Ratu river in the upper stream up to dividing point, EWH is about 35 km length and the extent of the watershed is about 91 km^2. The average gradient of the riverbed is 1/100 on this section. Width of the river changes dramatically below the EWH, where to the north of highway the width is about 600 meters, and below the highway the width has been extended to 2 to 3 km. The riverbed below the highway could be considered as the deposited area of the sediments. In 1993 July flood, the flooded area has been extended up to 20 km south of the down stream from the highway, Point A in Figure 6.2. This figure shows the Ratu riverbed gradient curve. The length of the

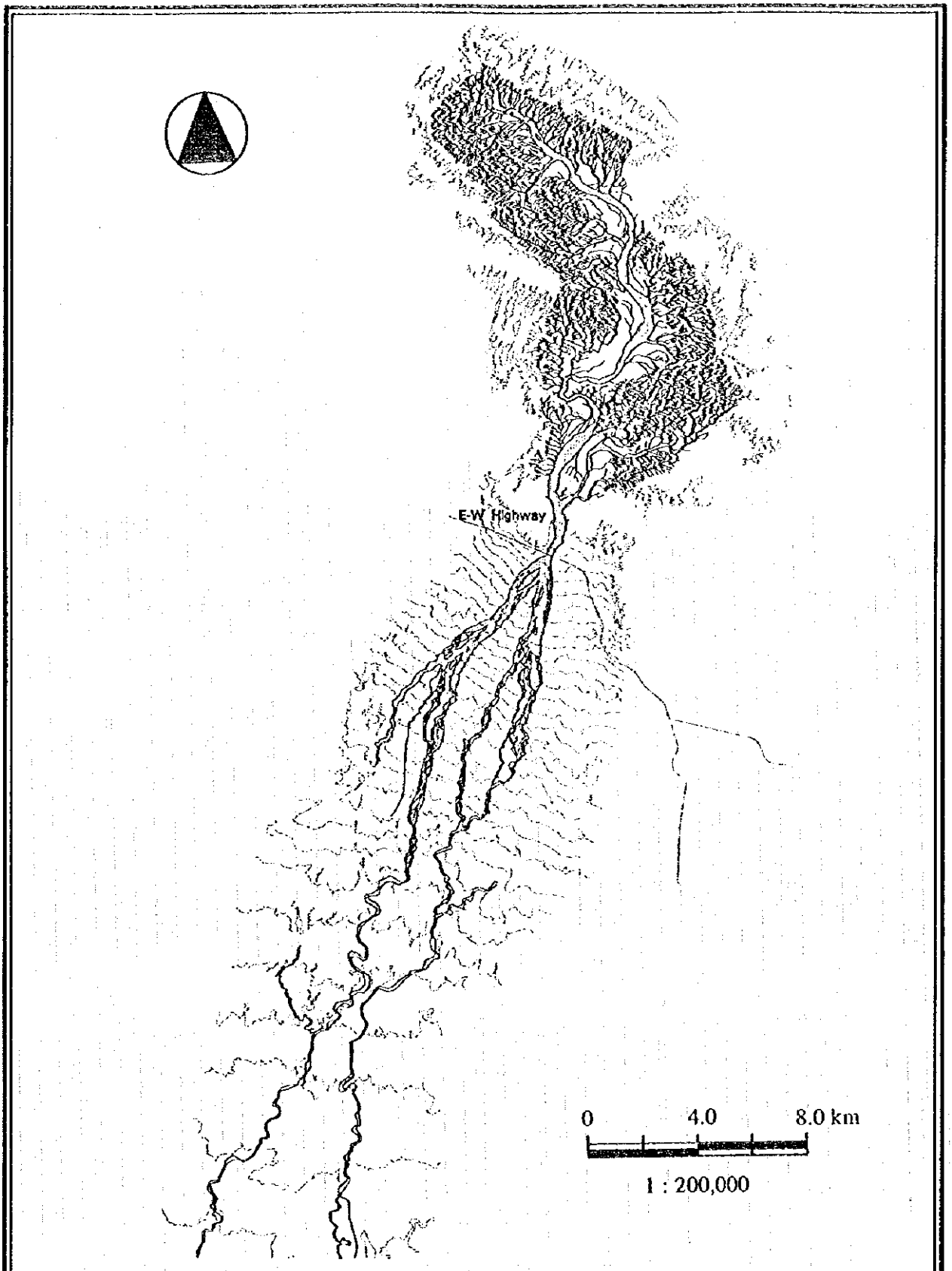

RESEARCH REPORT ON THE INVESTIGATION OF LANDSLIDE AND SOIL EROSION IN NEPAL USING REMOTE SENSING TECHNOLOGY	Figure 6.1 Geographical features of Ratu watershed
	JAPAN INTERNATIONAL COOPERATION AGENCY

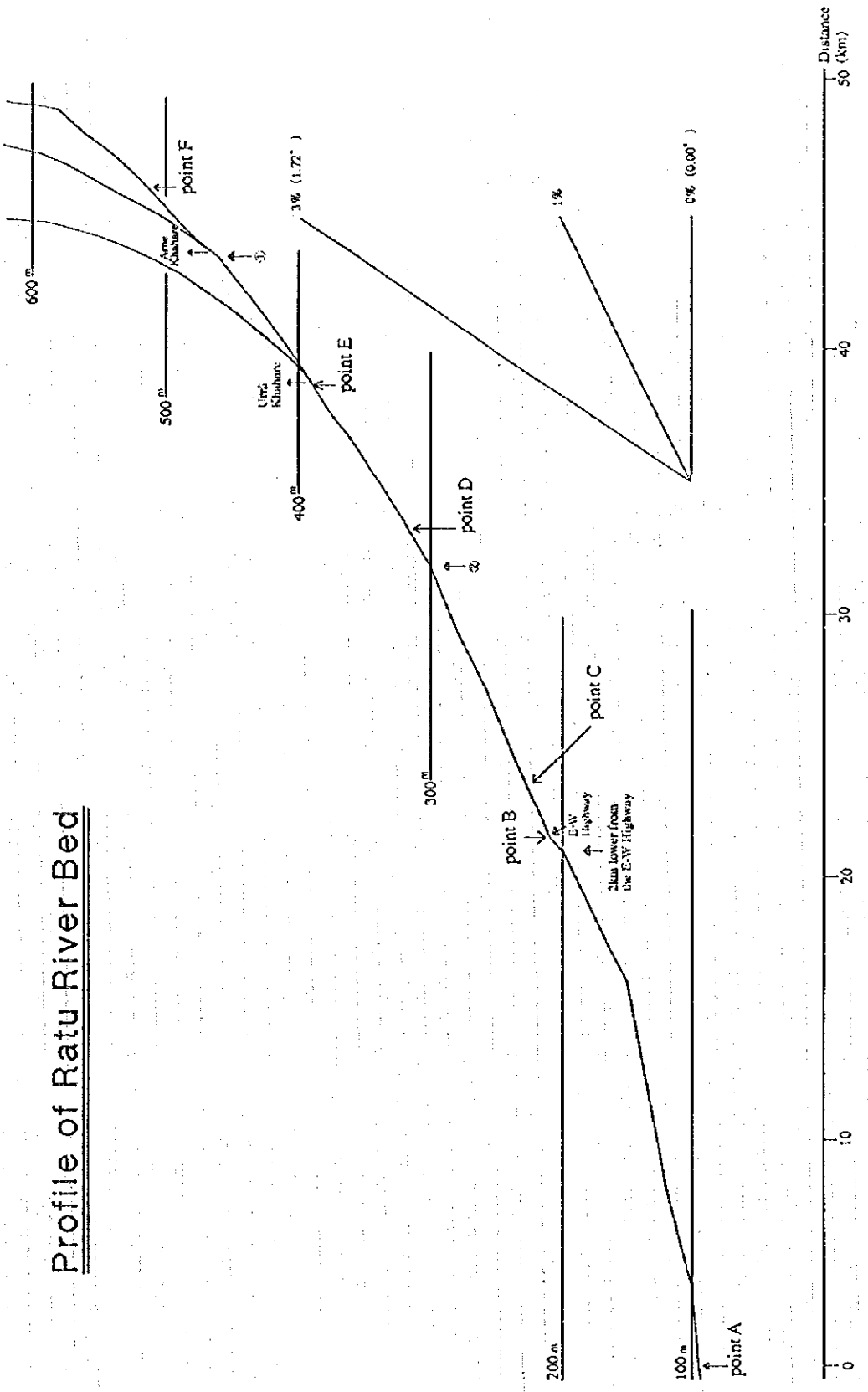

RESEARCH REPORT ON THE INVESTIGATION OF LANDSLIDE AND SOIL EROSION IN NEPAL USING REMOTE SENSING TECHNOLOGY

Figure 6.2
Profile of Ratu riverbed

JAPAN INTERNATIONAL COOPERATION AGENCY

river from A to its origin is about 55 km. The average slope of the riverbed is about 1/100. From point A to B, just below the highway, the gradient is about 1/200, and this area has become a large fan where much of the sediment is unloaded. The river gradient from EWH, Point B to the confluence point of Arne river is about 1/100. The gradient is 1/67 between the Arne confluence point and 1.9 km downstream from the source of the river. In the final 1.9 km of the river stretch the gradient changes to 1/9. The grain size analysis showed that the distribution of sediment size changes form coarse to fine towards lower reach of the Ratu river, Figure 6.3. This result shows the sediments are mainly transported by stream line flow, not by debris flow.

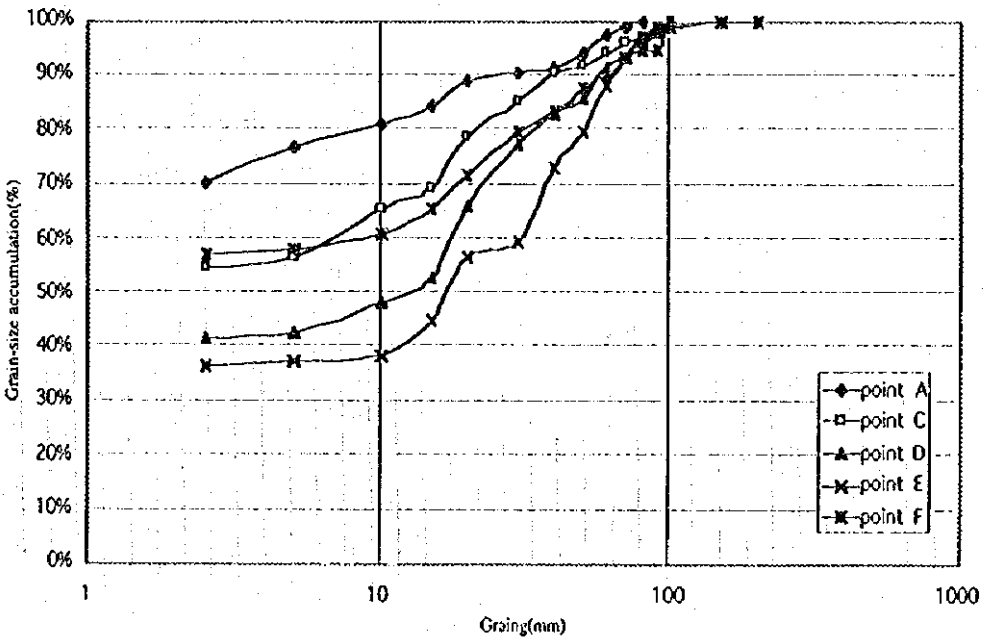

Figure 6.3 Grain size distribution in the Ratu river

Short sub-streams with higher gradient, and very flat riverbed is typical to the rivers originate in the Siwalik hills. With the increase of the gradient, the watershed becomes narrow. Further, the dendritic drainage pattern develops towards the upper stream of the River with the increase of riverbed gradient. These fact means that the soil erosion is high in the sub-streams. Upper reach

of the Ratu river up EWH functions as a sediment production and transport region, and lower stream below EWH acts as the floodplain.

Combination of NE-SW oriented main ridges at an altitude of 600~800 meters and sub-ridges oriented perpendicular to the main ridges are main landform characteristic of this watershed. Land form of Ratu watershed is consisted of gentle hills, with a peak of 708 meters above mean sea level, and river stream is controlled by their ridges.

Geology of Ratu watershed is consisted of Siwalik group, middle Miocene ~ Pleistocene, tertiary. Upper Siwalik formation, Middle Siwalik formation and Lower Siwalik formation distributed in the northern part of the watershed from the standard point EWH. Upper Siwalik formation widely distributed up to the confluence point with Urra river from the source. This formation is consisted of sand stone layer of yellowish brown and irregularly interbeded silt layer within boulders layer. Brown's unconsolidated Boulder, max. 30 cm, average 5 cm constitutes boulders layer. Middle Siwalik formation is distributed up to 2 km in the upper stream from EWH from the Urra confluence point. This formation is consisted of fine ~ coarse sand stone and silt layer. This layer is massive and formed with semi-consolidated ~ unconsolidated sediments with gray color. Dry rocks of this formation look gray-white color. Lower Siwalik formation is distributed near EWH, and it is consisted of fine sand stone ~ silt stone layer of yellow gray ~ reddish gray color. As the rocks in this formation are in the process of cementation, they are the most hardest in the Ratu watershed. Geological structure of these Siwalik group shows that the strike is North West - South -East and the dip is changeable. In addition to these, it is pointed that this area is moved by Neo-tectonics movements, Iwata (1988), and Matsuda (1983) showed that the Siwalik area involving Ratu watershed are Neo-tectonic areas on comparison of many terraces. Nakata (1988) estimated the uplift speed along Timai river of East Siwalik is 1.0~1.7 m /1000 year.

6.1.2 Characteristics of Soil Erosion in the Ratu Watershed

During the field visits, river characteristics and soil production was examined in the main river and some of the sub-streams. In establishing the physical characteristics and the nature of the soil erosion of the study area these field investigation were extrapolated integrating other information, such as geological, and topographical maps, and publications.

The average length of sub-streams of this area ranges from 800 meters to 1 km. At the confluence of most of the sub-streams with the main-stream, large fans about 10 ~ 15 meter in radius exited where eroded materials are deposited. Cliffs from the riverbed exit along the sub-streams. Figure 6.4 is a plain sketch map of typical sub-stream. Figure 6.5 shows a profile of a sub-stream riverbed. Along the sub-stream landslides and many slope failure are found.

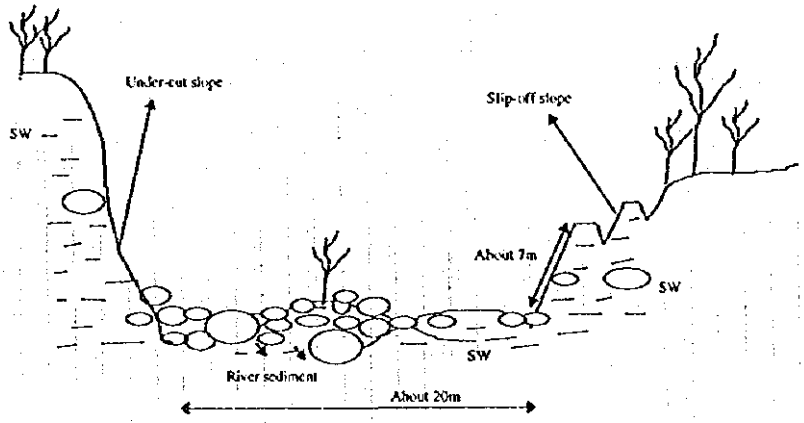

Figure 6.6 Cross section of the sub-stream in the downstream of Ratu river

Further the vertical cliff with several meters high was surrounded the sub-streams, like vertical walls. Sub-stream bed gradient shows 1/4~1/7 and the gradient increase up to 1:0.3 towards the source point.

Conceptual cross section of downstream portion of a sub-stream is shown in Figure 6.6. The average riverbed width was about 20 meters. Cliffs consisted

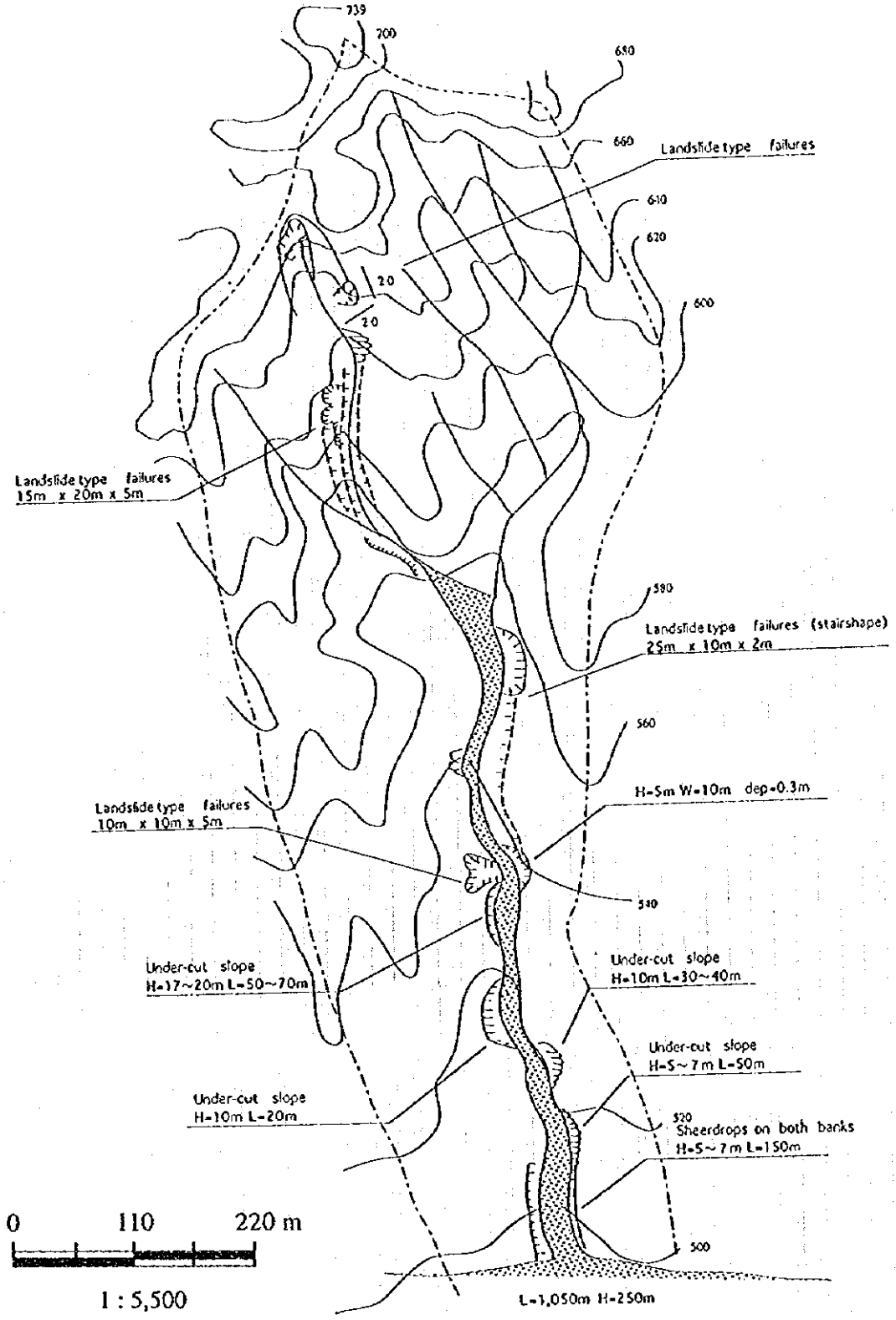

RESEARCH REPORT ON THE INVESTIGATION OF LANDSLIDE AND SOIL EROSION IN NEPAL USING REMOTE SENSING TECHNOLOGY	Figure 6.4 Conceptual geomorphological map of sub-stream
	JAPAN INTERNATIONAL COOPERATION AGENCY

RESEARCH REPORT ON THE INVESTIGATION OF LANDSLIDE AND SOIL EROSION IN NEPAL USING REMOTE SENSING TECHNOLOGY	Figure 6.5 Riverbed profile of a sub-stream
	JAPAN INTERNATIONAL COOPERATION AGENCY

of Upper Siwalik formation with 6~7 meters high exist both side of the stream. Two types of failures can be observed on these cliffs. The first type of failures are occurred by erosion of stream on undercut slopes (after herein C-1). This failure is caused the erosion on under portion of the cliff. The failure depth was about 30 cm. The second type was the earth topple failure type (after herein C-2). In this type, 50 cm thickness strata slumping fall into river bed. Gap cracks and open cracks behind failures distributed along the stream bed can be observed. These cliffs are created by eroding deposited material over the fan by the discharge of river flow during the rainy season.

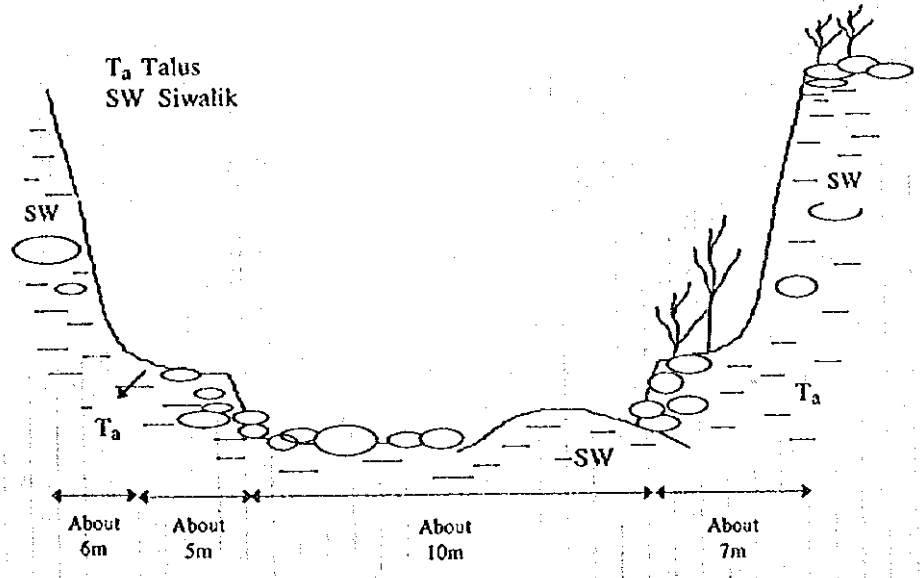

Figure 6.7 Cross section of the sub-stream in the upper portion

On the middle and upper stream portion of sub-stream, width of channel become narrower averaging 5 ~ 10 meters. Flat areas like terrace exist both sides of these channels, and cliffs having 1:0.3 gradient, and height about 15 ~20 meters exist on the hill side, Figure 6.7. The cliff consisted of Upper Siwalik sediments that random inclusion of big boulders in the size of human head in the matrix of very fine sand ~ cobble, vertically eroded by rain fall and wind (herein referred to as erosion type A). Erosion depth is 20 cm and erosion extends up to 20% of the surface area of the cliff. The most of debris

produced from the cliff fall directly into the stream bed and the rest fall into the stream bed after the formation of cone fan on the flat area. Failure of the flat area like terraces by the erosion was also visible along the middle ~ upper stream (herein referred to as erosion type B). Flat area is consisted of fine sand and silt sediments including 30 ~ 40 cm diameter of the boulders. The failure depth is about 10 cm. Landslide failures are occurred on the under cut slope of the middle ~ upper sub stream (herein referred to as erosion type D). This failure type has the distinct main scarp and many open cracks in the displaced material. Width of a slide is about 20 meters, and falls into the stream in the shape of horseshoe. This failure material are consisted of the cobble ~ boulder of Upper Siwalik formation. For this reason landslide failure fall little by little into the river.

The results of grain size analysis of the sub stream is shown in Figure 6.8. The figure shows that the distribution of sediment size changes also from coarse to fine towards lower reach of the sub stream.

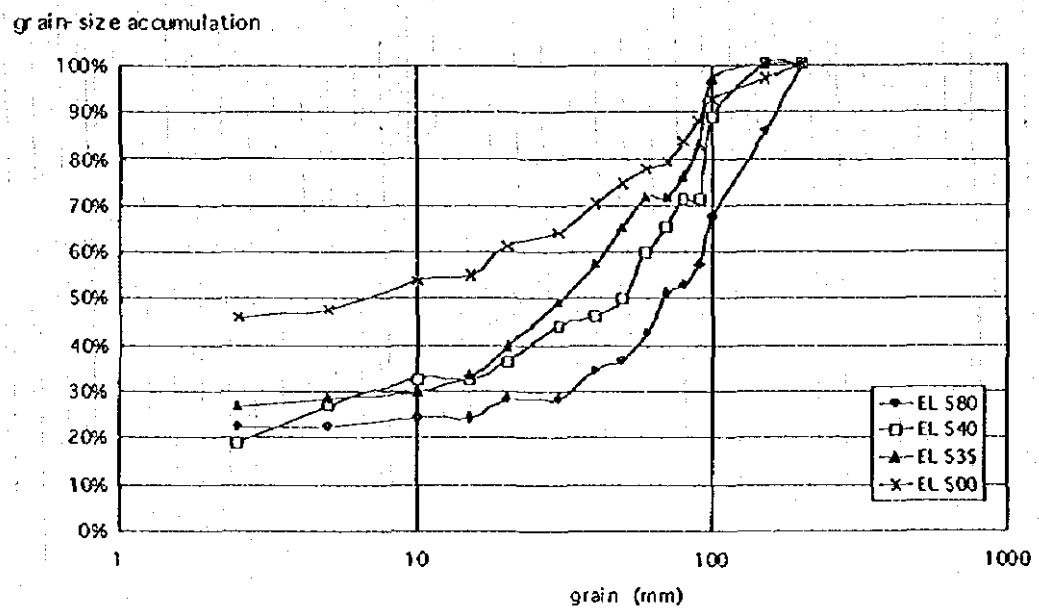

Figure 6.8 Grain size distribution in the sub stream

Considering these phenomena, the soil erosion and transportation in the sub stream can be considered as follows;

(1) Initially, the main cause of soil production may be uplift movement. Because, in the first place the 1:0.3 gradient cliffs almost vertical exist anywhere despite the geology of semi-consolidated ~ unconsolidated sediments of Upper Siwalik formation. This phenomena may be caused by high speed uplift and erosion. In the second place, meandering and degradation of sub-streams is remarkable. Flat areas similar to terraces are found in the middle upper stream and meandering are not formed only by erosion. In the third place, local residents witnessed for frequent earthquakes occur in this area. In the forth place, many geologists documented the uplift phenomenon and the quantity in the Siwalik hills. These factors are strong evidences to consider that the root of soil production in this area is a consequence of the uplift movement.

(2) The eroded material due to very steep gradient slope, and stresses as a consequence of uplift movement contribute for deposition in the form of failures due to rainfall, deposit on stream, by earthquakes or wind (A). The produced debris tentatively deposit on the flat area. These deposits are eroded or washed out by rainfall and stream water (B). Depend on the discharge capacity of running water during the rainy season, these deposited material are transported along the sub-streams carrying the grains that are moveable by the stream force.

(3) Stream water erodes slopes and causes irregular failures adding sediments into the riverbed that is transportable with the running water(C-1, C-2, D).

By the repetition of these phenomena, sub-stream beds are eroded in order to and bank erosion continues to maintain the landform equilibrium. The present landform of sub-stream watershed is formed by these mechanism

6.1.3 Characteristic of Soil Transportation and Siltation in the Study Area

In Ratu watershed three times flood events are recognized; the flooding of 85, 93 and 95.

During the field survey, residents in the area were interviewed to identify the deformation of Ratu riverbed during flood events. The results of the survey can be summarized in the four points bellow;

In the first, the heavy rainfalls made irregular river bed degradation, and aggradation up to the confluence point with Urra river from the source. The deformation of river bed in this stretch was about 0.5 ~ 1.0 meter. In the second, after 93 flood event river bed has been aggraded by 0.5 meters to the confluence point with Urra river from the source. In the third, from the confluence point to the EWH the river bed has aggraded 0.5 meters per one flooding. In the forth, the flooding water might have caused undercutting erosion in the Ratu main stream channel.

By the aerial photograph survey, the scaled type sand bars can be observed in the Ratu main channel. This observation indicates that the stream way is changeable by rainfalls and the river bed has the trend of aggradation by the siltation and may be due to tectonic uplift. These phenomena coincides with the statements of residents in the area. Figure 6.3 shows the grain size distribution in the main channel changes form coarse to fine towards lower reach of the river. This indicates the main stream of Ratu river is functioning as a mode for soil transportation by stream line flow.

River stream has radially expanded to the down stream from the EWH. The pattern of the sand bars are also scaled. Figure 6.3 shows that average grain size distribution in the flooding area changes into 1 mm from 1.0 cm of the average grain size of the EWH. These facts indicate that the expansion of the stream width and the aggradation on the main streambed could have decreased the rapidity of stream flow. Stream velocity influences the distribution of the soil deposition, and the deposition take place with respect to

the velocity. Yamamoto (1988) showed the relation of grain size and the depth of stream water, Figure 6.9. This figure shows, that the velocity and the depth of the stream is very small under the very low gradient.

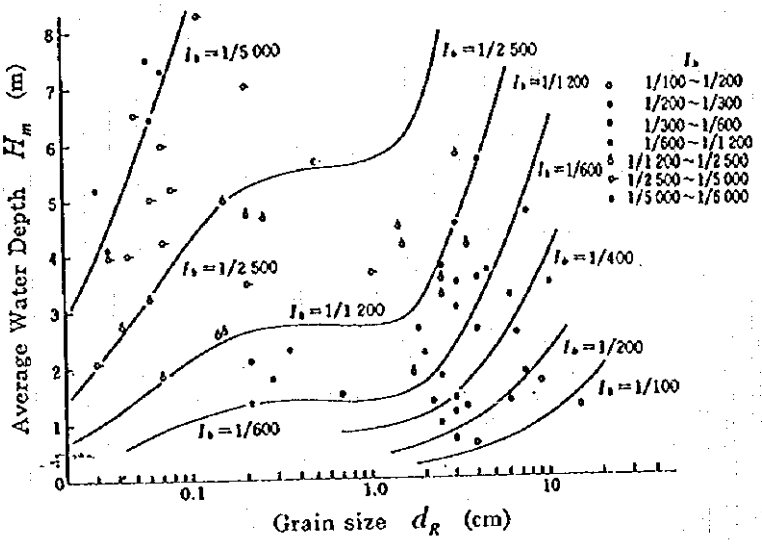

Figure 6.9 Stream depth Hm, DR and Ib

6.2 Flooding Volume on the Lower Stream from East -West Highway

It is required to estimate the deposit volume on the lower stream from East - West Highway after the 1993 flood for analysis of the soil production and the balance of deposit. As there are no data showing the flooded area and the amount of runoff, it was attempted to collect information that could help to establish the deposited volume in the Ratu floodplain.

Generally, stream water start to deposit sediments according to the capability of bed load transportation. After depositing more coarser sediment near EWH, the capability of bed load transportation capacity of stream become smaller due to expansion of the stream. As a consequence, particles of average diameter 1 mm or smaller are further washed out and deposited at the end of flooding area. During the sediment deposition, the distribution is controlled

by the capability of bedload transportation and the gradient of the river bed. Extensive field work and monitoring is required for detail investigation and establishment of the sediment transportation and deposition process in the downstream. For this reason, the analysis of the capability of bedload transportation can not be accomplished without long term observation, hence in the present research work attempt was made to evaluate the sediment volume after 1993 flood event on the flooding area from the results of field reconnaissance and satellite images.

In the west side of sub-stream riverbed, sediments have been deposited with an average width of 60 meters, and maximum width of 120 meters, where the average depth ranging form 0.3~0.5meters on the most lower portion of the flood plane. The width of the river channel is 130 ~140 meters and the width of stream way is about 20 meters in this section. Depth of sediments can be estimated as 2 ~ 3 cm. on the other sediment areas other than the riverbed from the observation in field and on the statements of the residents. River cross section is shown in the Figure 6.10. From this figure, it can be evaluated that the flooding volume at the time of flood event of 1993 may have reached at least to 32 m^2 at average river section. On the other hand , this reveals the stream had the capability to transport only a bedload of 32 m^3.

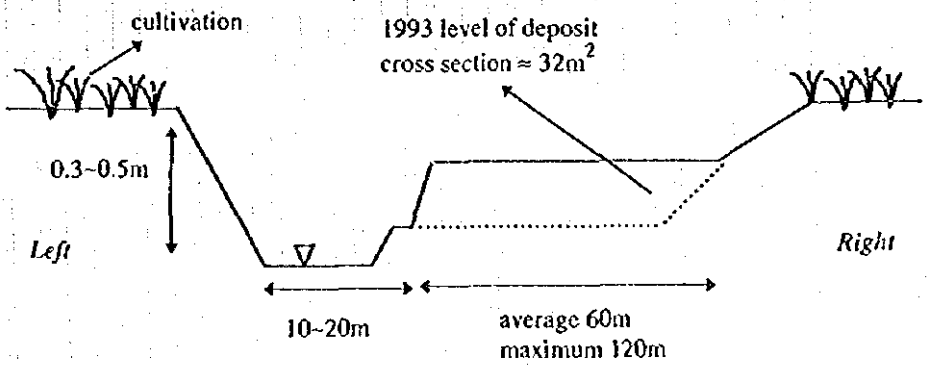

Figure 6.10 River cross section in the most lower part of the floodplain

The sediments produced and transported by Ratu watershed started to deposit radially after passing EWH. Flooding of this event has two main features.

Firstly, the flooding area can be divided into several ways along the streams from EWH. Secondly, the flooding existed along the stream. From satellite image the flooding area of 1995 was estimated as 9.601 km^2. From Figure 6.11 and Table 6.1, it was found that the total length of the stream is 41.7 km in the flooding area. The average width of stream changes to 150.6 meter, finally extended to 15 ~ 20 meters from 2 km near the EWH.

Table 6.1 Length and width of stream in the flood area

The width of branch channel in floodplain				Length of branch channels	
Number	width m	Number	width m	Number	length
No 1	372.0	No 11	180.0	S-1	5.7 km
No. 2	108.0	No. 12	126.0	S-2	15.1 km
No. 3	126.0	No. 13	60.0	S-3	9.2 km
No. 4	120.0	No. 14	162.0	S-4	11.7 km
No. 5	300.0	No. 15	30.0	Sum	41.7 km
No. 6	228.0	No. 16	276.0		
No. 7	198.0	No. 17	132.0		
No. 8	168.0	No. 18	48.0		
No. 9	120.0	No. 19	sum 2862		
No. 10	60.0	No. 20	mean 150.6		

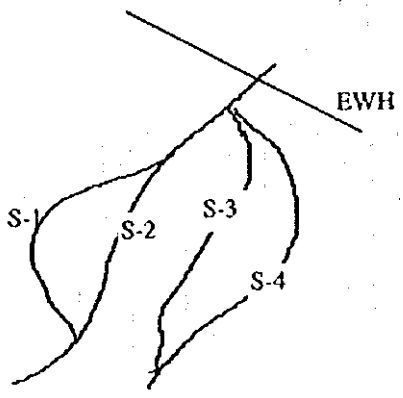

Then, assuming that the capability of bedload transportation estimated from the site reconnaissance equally distributed over the flooding area, flood

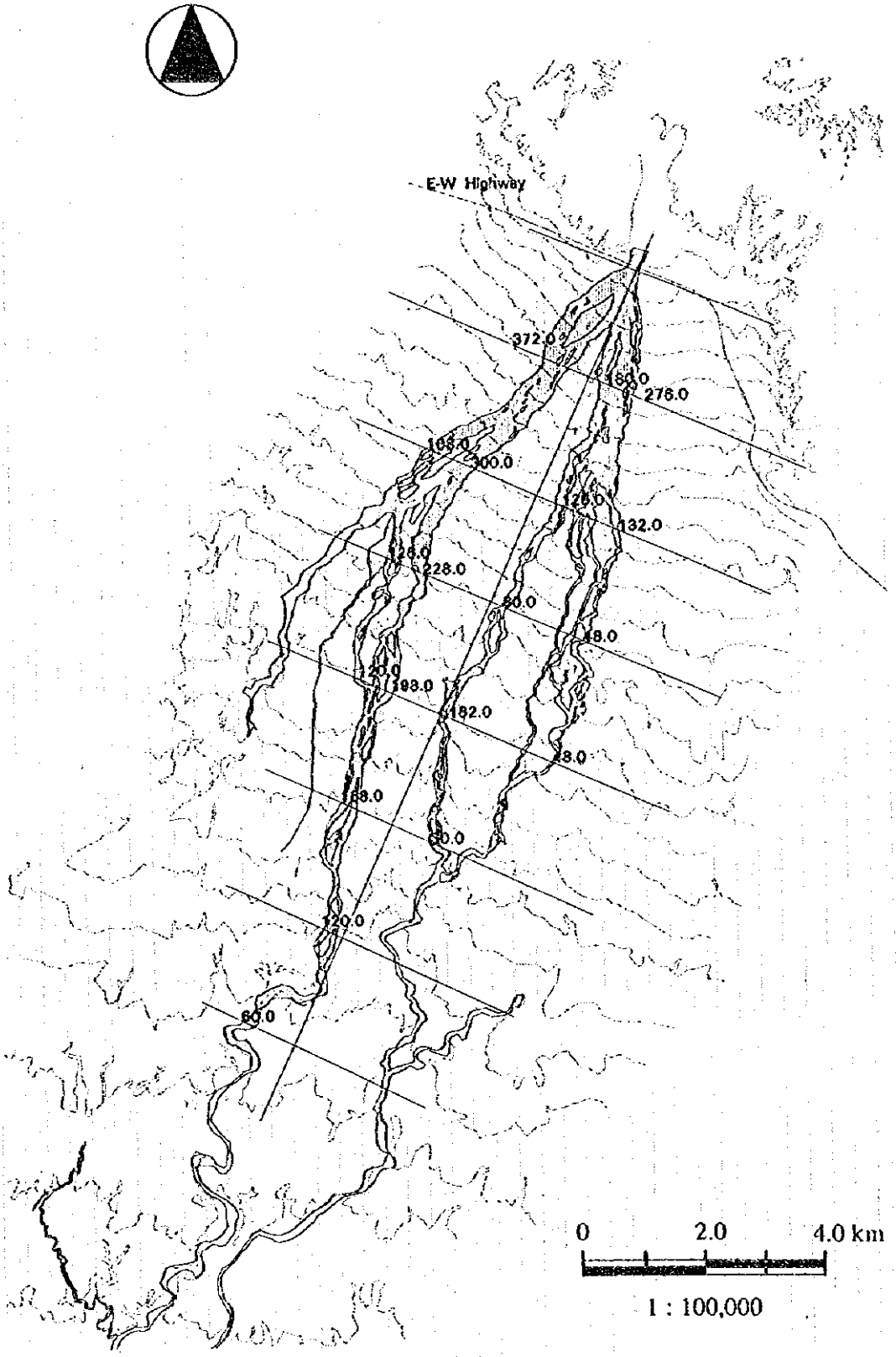

RESEARCH REPORT ON THE INVESTIGATION OF LANDSLIDE AND SOIL EROSION IN NEPAL USING REMOTE SENSING TECHNOLOGY	Figure 6.11 Main channel network in the Ratu river floodplain
	JAPAN INTERNATIONAL COOPERATION AGENCY

volume is calculated as below;

The stream has the 32 m^2 per meter of the capability of bedload transportation as long as the average depth of the flooding h is

$$30 = 240 \times h$$
$$h = 0.125m$$

Therefore, the flooded volume in the stream is

$$62{,}000 \times 0.125 \times 240 = 2{,}040{,}000m^3$$

Then the volume of the deposited materials is,

$$9.601 - 41.7 \times 0.1506 = 3.32 \text{ km}^2$$

Then the effective flooding area excluding the extent of the riverbed,

$$1{,}331{,}364 + 66{,}400 = 1{,}397{,}764m^3$$

about 1.40 million m^3 can be estimated as total flooding volume.

6.3 Soil Production Model and the Soil Balance

One of the purpose of this research is the application of satellite remote-sensing for debris control analysis. In this area there are no valid data for this analysis. Therefore, it is required to estimate the production of sediment of this area by some other mean. Also, the volume estimated must be checked by establishing a soil balance model. This will facilitate the validation and confirmation of the estimated volume of production.

For this, it is required to calculate the soil production volume in the Ratu watershed. Further, the soil production volume calculated must be validated by the analysis of soil balance.

The data of soil production volume and the deformation volume of the bed during the certain sections are necessary to establish the balance of sediment in the Ratu watershed. Although the flooding volume could be estimated from the result of site reconnaissance and satellite images, soil production volume still be an unknown. In this section, attempt was made to analyze the sediment balance by establishing a soil production model and evaluating the soil balance of the Ratu watershed on the information of the river bed deformation gathered from people living in the area.

6.3.1 Soil Production Model of Ratu watershed

Soil erosion is mainly occurred in the upper sub-streams of the watershed. It can be assumed that the present soil production situation is relics of the 93 flood event, therefore 93 soil production volume can be calculated by modeling of five failure patterns described in section 6.1.2. Given this condition, method that followed to estimate 1993 flood event soil production volume is described below.

The mechanism of soil production in the Ratu watershed can be described in five types as referred to as A, B, C-1, C-2 and D, in section 6.1.2. These five types of soil production in the Ratu watershed occurs on the slope along the stream way. That is to say, the soil production in this watershed can be expressed by a function of stream way with an invariant value for the height, width and appearance ratio of five failure types described in section 6.1.2.

Then, representing "V_A,V_B,V_{C1},V_{C2},V_D " as the soil production volume for each type recognized, the total V_{total} can be represented as,

$$V_{total} = \sum V_A + \sum V_B + \sum V_{C1} + \sum V_{C2} + \sum V_D$$

Here, V_A,V_B, ,V_D are the production volume of the failure types located on

the middle ~ upper sub-stream and V_{C1} and V_{C2} represent the production volume of the failure types located on the lower sub-stream. If the total length of sub-stream is described as L, and the length of the middle ~ upper and the lower sub-stream as L1, L2, the relation of stream length can be expressed as;

$$L = L_1 + L_2$$

The heights, gradient, depth and five types of failures appearance ratio with respect to each of the failure types are summarized in Table 6.2.

Table 6.2 Failure features in the sub-stream

	Height $h_{(m)}$ (m)	Gradient	Depth w_m (m)	Appearance Ratio to the stream P(%)
A	10~15m (12m)	60°~ Vertical	0.2	L_2 x 15% x 50% x 200%
B	2~3m (7m)	Vertical	0.2	L_2 x 15% x 200%
C	5~8m (7m)	Vertical	0.3	L_1 x (5/28 + 150/1400)
D	5~8m (7m)	Vertical	2	L_1 x 25/1400
E	15m	60°~ Vertical	2	L_2 x 10%

From Table 6.2 we can calculate the total soil production volume in the watershed as follows;

V_A = L_2 x 15% x 50% x 200% x 12 x 0.2

V_B = L_2 x 15% x 200% x 2.5 x 2.5 x 0.2

V_{CI} = L_1 x (5/28 + 150/1400) x 7 x 0.3

V_D = L_1 x (25/1400) x 7 x 2

V_{CI} = L_2 x 10% x 15 x 2

In Ratu watershed eighty five sub streams are recognized. Then after calculating L1, L2 through drainage system data inputted to GIS, the total volume can be calculated as follows;

$$
\begin{aligned}
V_{total} &= \sum V_A + \sum V_B + \sum V_{C1} + \sum V_{C2} + \sum V_D \\
&= 0.36L_2 + 0.5L_2 + 0.6L_1 + 3L_2 + 0.25L_1 \\
&= 0.85L_1 + 3.86L_2 \\
&= 0.85 \times 92,162 + 3.86 \times 573,558 \\
&= 2,292,272(m^3)
\end{aligned}
$$

The resulted volume 2.3 million m^3 is the estimated soil yield for the year 1993 flood event.

6.3.2 The Soil Balance of the Watershed

The balance of produced soil in the Ratu watershed can be analyzed on the calculation of the cumulative volume, the runoff volume and the deformed volume of the main streambed per each section. Each sections are shown in the Figure 7.6. This shows the results of soil production of each section estimated by the above model. The area of Ratu river channel was calculated by TM satellite image of 95 March. The deformation volume of the main stream bed of each section was estimated by the depth changes information given by people in the area. The sediment balance analysis is shown in Table 6.3.

In this table we considered the volume of stream way was transported to the down section after the flooding. The estimated flooding volume below EWH is about 1.416 million m^3.

These result was almost agreed with the 1.39 million m^3 gotten from site reconnaissance and satellite image analysis. Therefore, 2.29 million m3 of total soil production can be considered as the soil yield for a flood event in the order of 1993 July.

Table 6.3 Soil balance in the Ratu watershed

Section	Estimated 93 flood volume	Volume flow form upper section	Cumulative total at standard points	change of sediment volume	sectional depth x width	sediment flow at standard points	channel surface area	Residents statements
F to upper	320,000	0	320,000	-155,700		475,700	0.156	1 m down
E to F	250,000	475,700	725,700	-431,100		1,156,800	0.431	1 m down
D to E	460,000	1,156,800	1,616,800	547,200	51,000	1,120,600	1.094	0.5m up
C to D	780,000	1,120,600	1,900,600	1,537,650	1,000,000	1,362,950	3.075	0.5 m up
EWH to C	480,000	1,362,950	1,842,950	627,300	200,000	1,415,650	0.627	1 m up
Total	2,229,000	4,116,050	6,406,050	2,125,350	1,251,000	flooded volume 1,415,650		